The Plant Cell, Vol. 21: 3473–3492, November 2009, www.plantcell.org

Photosynthetic Redox Imbalance Governs Leaf Sectoring in the *Arabidopsis thaliana* Variegation Mutants *immutans*, *spotty*, *var1*, and *var2*[W]

Dominic Rosso,[a] Rainer Bode,[a] Wenze Li,[a] Marianna Krol,[a] Diego Saccon,[a] Shelly Wang,[a] Lori A. Schillaci,[a] Steven R. Rodermel,[b] Denis P. Maxwell,[a] and Norman P.A. Hüner[a,1]

[a] Department of Biology and the Biotron, University of Western Ontario, London, ON, Canada N6A 5B7
[b] Department of Genetics, Development, and Cell Biology, Iowa State University, Ames, Iowa, 50011

We hypothesized that chloroplast energy imbalance sensed through alterations in the redox state of the photosynthetic electron transport chain, measured as excitation pressure, governs the extent of variegation in the *immutans* mutant of *Arabidopsis thaliana*. To test this hypothesis, we developed a nondestructive imaging technique and used it to quantify the extent of variegation in vivo as a function of growth temperature and irradiance. The extent of variegation was positively correlated (R^2 = 0.750) with an increase in excitation pressure irrespective of whether high light, low temperature, or continuous illumination was used to induce increased excitation pressure. Similar trends were observed with the variegated mutants *spotty*, *var1*, and *var2*. Measurements of greening of etiolated wild-type and *immutans* cotyledons indicated that the absence of IMMUTANS increased excitation pressure twofold during the first 6 to 12 h of greening, which led to impaired biogenesis of thylakoid membranes. In contrast with *IMMUTANS*, the expression of its mitochondrial analog, *AOX1a*, was transiently upregulated in the wild type but permanently upregulated in *immutans*, indicating that the effects of excitation pressure during greening were also detectable in mitochondria. We conclude that mutations involving components of the photosynthetic electron transport chain, such as those present in *immutans*, *spotty*, *var1*, and *var2*, predispose *Arabidopsis* chloroplasts to photooxidation under high excitation pressure, resulting in the variegated phenotype.

INTRODUCTION

Plants sense light through an array of photoreceptors, including phytochromes (Rockwell et al., 2006; Bae and Choi, 2008), cryptochromes (Li and Yang, 2007), and the more recently discovered phototropins (Christie, 2007) that are critical for plant growth and development. However, in addition to the requirement for photoreceptors sensitive to spectral quality, the oxidation-reduction (redox) state of photosynthetic electron transport (PET) has been shown to act a sensor of cellular energy status (Hüner et al., 1998; Giraud et al., 2008; Murchie et al., 2009). Imbalances in the redox state of PET may occur whenever the absorption and transformation of light by the extremely fast, temperature-insensitive photochemical reactions of photosynthesis either exceed the capacity to use the photosynthetic electrons for reductive C, N, and S metabolism and/or exceed the capacity of the photosynthetic apparatus to dissipate excess energy non-photochemically as heat (Hüner et al., 1998; Pfannschmidt, 2003; Ensminger et al., 2006; Wilson et al., 2006; Murchie et al., 2009).

The redox state of PET has been shown to influence a diversity of phenomena from altering the excitation distribution between photosystems through state transitions controlled by *STN7*, a chloroplast thylakoid protein kinase in *Arabidopsis thaliana* (Rochaix, 2004; Kargul and Barber, 2008), to changes in organellar gene expression (Pfannschmidt et al., 1999; Pfannschmidt, 2003) and nuclear gene expression through retrograde regulation (Pfannschmidt, 2003; Fernández and Strand, 2008; Woodson and Chory, 2008; Pesaresi et al., 2009; Pfannschmidt et al., 2009), to changes in plant growth habit and morphology (Gray et al., 1997). Furthermore, tobacco (*Nicotiana tabacum*) plants deficient in ferredoxin-NADP(H) reductase exhibit a yellow-green phenotype due to the overreduction of the intersystem PET chain. The extent of this phenotype is directly dependent upon the irradiance to which the plants are exposed (Palatnik et al., 2003). Consequently, it has been suggested that the chloroplast has a dual role. Not only does it function as the primary energy transducer in all photoautotrophs, it also functions as a sensor of environmental change (Hüner et al., 1998; Pfannschmidt, 2003; Wilson et al., 2006; Bräutigam et al., 2009; Murchie et al., 2009).

Early research with green algae indicated that a key sensor was the redox-state of plastoquinone (PQ), a mobile electron carrier that shuttles electrons from photosystem II (PSII) to the cytochrome b_6/f complex (Escoubas et al., 1995; Maxwell et al., 1995b; Wilson et al., 2003). This was based on experiments where the characteristic, yellow-green, high light phenotype brought about by acclimation to high irradiance could be mimicked by chemically modulating the redox status of the intersystem PQ pool with the electron transport inhibitor 2,5-dibromo-3-methyl-6-isopropylbenzoquinone (DBMIB) in *Dunalliela tertiolecta* (Escoubas

[1] Address correspondence to nhuner@uwo.ca.
The author responsible for distribution of materials integral to the findings presented in this article in accordance with the policy described in the Instructions for Authors (www.plantcell.org) is: Norman P.A. Hüner (nhuner@uwo.ca).
[W] Online version contains Web-only data.
www.plantcell.org/cgi/doi/10.1105/tpc.108.062752

et al., 1995) and *Chlorella vulgaris* (Wilson et al., 2003). Since DBMIB inhibits the oxidation of plastoquinol (PQH_2) by the cytochrome b_6/f complex, PSII keeps the PQ pool reduced in the light. This induces the high light phenotype, which is characterized by low chlorophyll content per cell, high chlorophyll *a*/*b* ratio (>10), accumulation of the carotenoid binding protein, but suppression of both Lhcb2 accumulation and *Lhcb2* expression, the nuclear gene that encodes the major PSII light-harvesting antenna polypeptide (Hüner et al., 1998).

While low temperature does not affect the rate of light absorption, it severely restricts the rate of downstream, enzyme-catalyzed reactions. This restricts the capacity to use NADPH and ATP, the products of the PET, thus causing an overreduction of the PQ pool due to negative feedback. As a consequence, the yellow, low-temperature phenotype is indistinguishable from the phenotype observed in the presence of DBMIB (Maxwell et al., 1995a; Wilson et al., 2003). By contrast, since DCMU prevents the exit of electrons from PSII into the PQ pool, photosystem I (PSI) is able to keep the PQ pool oxidized in the light. Under these conditions, cells exhibit a normal green phenotype that is associated with high chlorophyll content per cell, low chlorophyll *a*/*b* ratio (3.0 to 3.5), high levels of *Lhcb2* expression, and Lhcb2 accumulation (Escoubas et al., 1995; Wilson et al., 2003). This phenotype is mimicked by growth at either low irradiance or high temperature in *C. vulgaris* (Maxwell et al., 1995a; Wilson et al., 2003).

More recent research in *Arabidopsis* suggests that redox factors on the acceptor side of PSI may be important (Dietz, 2008). These and additional signals, including the precursor of chlorophyll synthesis, magnesium protoporphyrin (Strand et al., 2003), and reactive oxygen species (ROS) generated by the PET (Meskauskiene et al., 2001; op den Camp et al., 2003), may constitute a complex network of signals involved in the retrograde pathway of communication from the chloroplast to the nucleus (Koussevitzky et al., 2007; Fernández and Strand, 2008; Woodson and Chory, 2008). However, the putative role of Mg-protoporphyrin in retrograde signaling remains equivocal (Mochizuki et al., 2008; Moulin et al., 2008). Genetic analyses in *Arabidopsis* has identified STN7 (Bellafiore et al., 2005; Bonardi et al., 2005) as a chloroplast protein kinase involved in redox signaling essential for state transitions and photosynthetic acclimation (Pesaresi et al., 2009). However, the exact nature of the mechanisms by which the redox state of the chloroplast is signaled to the nucleus resulting in altered gene expression remains largely unknown.

Changes to the redox state of the PET chain are reflected in alterations to the excitation pressure of PSII. Excitation pressure can be formally defined as the relative measure of reduction state of Q_A, ($[Q_A^-]/[Q_A] + [Q_A^-]$) (Dietz et al., 1985; Hüner et al., 1998), the first stable electron acceptor of PSII. Excitation pressure can be measured noninvasively in intact tissues using chlorophyll *a* fluorometry (Krause and Weis, 1991) to measure the parameter 1-qP (Dietz et al., 1985; Maxwell et al., 1994; Adams et al., 1995). Photoautotrophs are in photostasis when the photochemistry induced by the absorption of light is balanced either by use of photosynthetically generated electrons through metabolism and growth or through the capacity to dissipate excess energy as heat through nonphotochemical quenching (Figure 1) (Hüner et al., 2003). Under such conditions, excitation pressure is low, the PQ pool is in the oxidized state, and the organism exhibits a normal, green, low excitation pressure phenotype.

However, myriad environmental stresses, including high irradiance (Escoubas et al., 1995), low temperature (Maxwell et al., 1995a, 1995b; Wilson and Hüner, 2000; Wilson et al., 2003),

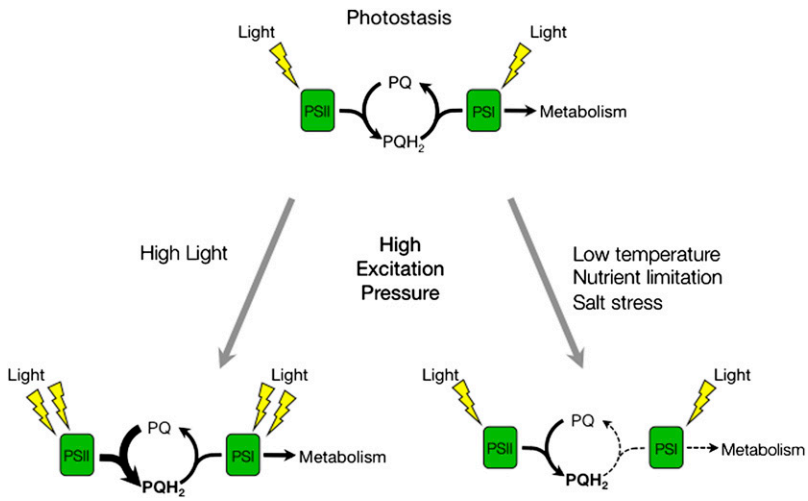

Figure 1. The Redox State of the PQ Pool Is a Sensor of Environmental Change.

During steady state photosynthesis, the diffusion-dependent oxidation of PQH_2 is considered the rate-limiting step of PET. At photostasis (top), the rate of reduction of the PQ pool by electrons from PSII is balanced by its oxidation by PSI and the demands of downstream metabolism. Exposure of plants to high light (bottom left) results in PQH_2 accumulation, which is reflected by increased excitation pressure on PSII. High excitation pressure conditions can be also mimicked by other environmental conditions (bottom right) that limit the rate of the oxidation of the PQ pool by inhibiting downstream metabolism that consumes the electrons generated by PET.

nitrogen deficiency (Cruz et al., 2003), and salt stress (Huang et al., 2005) increase excitation pressure due to energy imbalances between photochemistry and cellular energy use (Figure 1). In the single-cell green algae, *C. vulgaris*, *Dunaliella salina*, and *D. tertiolecta* (Escoubas et al., 1995; Maxwell et al., 1995a, 1995b) as well as the cyanobacterium *Plectonema boryanum* (Miskiewicz et al., 2000, 2002), this typically results in a high excitation pressure phenotype characterized by a decrease in chlorophyll per cell, a decreased abundance of pigments associated with the light-harvesting antenna, and a decreased photosynthetic efficiency typically associated with photoacclimation. These algae and *P. boryanum* adjust the structure and composition of light-harvesting complex II and phycobilisomes, respectively, reflecting their acclimation response to high excitation pressure.

The variegated phenotype is characterized by distinct green and white sectored leaves (Rodermel, 2001, 2002; Miura et al., 2007). The green sectors contain normal chloroplasts, whereas the white sectors contain plastids devoid of chlorophyll and/or carotenoids (Rodermel, 2002; Miura et al., 2007). Variegated plants include the *immutans* (*im*) mutant of *Arabidopsis*, which was isolated and preliminarily characterized nearly 50 years ago (Rédei, 1963, 1975; Röbbelen, 1968). *im* is the result of a recessive mutation of the nuclear gene *IM* (Carol et al., 1999; Wu et al., 1999). Recent in vitro and in vivo evidence indicate that IM may be the elusive plastid terminal oxidase (PTOX), an ancillary component of the PET chain that is involved in the chlororespiratory pathway (Cournac et al., 2000; Josse et al., 2000, 2003; Joët et al., 2002; Peltier and Cournac, 2002; Fu et al., 2005; Shahbazi et al., 2007). It was first proposed by Bennoun (1982) that, during chlororespiration, reducing equivalents from the stroma are oxidized by an NAD(P)H dehydrogenase that in turn reduces the PQ pool. The function of IM in this chlororespiratory pathway would be to mediate the oxidation of plastoquinol (PQH_2) and the concomitant reduction of O_2 to water.

Chloroplasts and mitochondria represent the major redox compartments of plant cells that can communicate through the complex network of C- and N-metabolic pathways. Consequently, plant cellular energy metabolism involves the integration of light-dependent, photosynthetic redox reactions with the light-independent respiratory redox reactions of mitochondria (Noctor et al., 2007). The mitochondrial alternative oxidase (AOX) is upregulated under stress conditions and oxidizes the ubiquinone pool of the mitochondrial electron transport chain and lowers the potential for ROS production (Maxwell et al., 1999; McDonald, 2008). IM exhibits 37% sequence identity to AOX (Wu et al., 1999). Consequently, it was suggested that IM, like AOX, acts as an electron transport safety valve (Niyogi, 2000). Under stress conditions when the PET chain becomes overly reduced, IM may act as an alternative electron sink that, by consuming excess photosynthetically generated electrons, would minimize the formation of ROS (Niyogi, 2000). PTOX has been reported to reduce oxygen and was suggested to play an important photoprotective role in the high alpine plant species *Ranunculus glacialis* acclimated to low temperature (Streb et al., 2005). Furthermore, Stepien and Johnson (2009) reported that PTOX acts as an alternative electron sink in the salt-stressed halophyte *Thellungiella*. These effects were accompanied by a significant increase in the relative abundance of PTOX in *R. glacialis* (Streb et al., 2005) and *Thellungiella* but not in *Arabidopsis* (Stepien and Johnson, 2009). These data support the role of IM/PTOX as an alternative electron sink in alleviating overreduction of the PQ pool under unfavorable environmental conditions where PSI is limited on the acceptor side.

However, recent research comparing the function of IM in a knockout mutant as well as in overexpressing lines of *Arabidopsis* has shown that modulation of *IM* expression and polypeptide accumulation does not alter the flux of intersystem electrons reaching PSI during steady state photosynthesis nor does the presence or absence of IM affect sensitivity to photoinhibition in *Arabidopsis* (Rosso et al., 2006). Moreover, through meta-analyses of published *Arabidopsis* microarray data, Rosso et al. (2006) reported that *IM* expression was insensitive to a range of abiotic stresses. Taken together, these results do not support the model of IM as a safety valve to regulate the redox state of the PQ pool during stress and acclimation in fully developed *Arabidopsis* leaves. By contrast, the meta-analysis revealed that *IM* did appear to be strongly regulated by development in *Arabidopsis* (Rosso et al., 2006). This is consistent with the observations of Aluru et al. (2001, 2009) who suggested that IM is required to protect against the potential for photooxidation during the development of chloroplasts, amyloplasts, and etioplasts.

Wu et al. (1999) proposed that the presence of white sectors in *im* plants occurs because IM plays a critical role in carotenoid biosynthesis due to its ability to oxidize the PQ pool. Briefly, a key enzyme in carotenoid synthesis is phytoene desaturase, which catalyzes the oxidation of phytoene to z-carotene, and this requires electron donation to PQ. The subsequent processing of z-carotene leads to the biosynthesis of the complete complement of carotenoids, including β-carotene, lutein, and zeaxanthin, which are required to protect the photosynthetic apparatus from photooxidation. By acting as a plastoquinol oxidase, IM helps to facilitate phytoene desaturase function. If the PQ pool remains reduced due to the lack of IM, carotenoid biosynthesis is blocked at the phytoene desaturase step, phytoene accumulates, and photobleaching results from an increase in chloroplastic ROS (Wetzel et al., 1994; Wu et al., 1999). Consistent with the notion that white sectoring is triggered by photooxidation (Aluru et al., 2009) is the fact that the variegated phenotype can be suppressed in *im* plants when grown under low-light conditions (Rédei, 1963; Wetzel et al., 1994; Aluru and Rodermel, 2004; Rosso et al., 2006).

We recently discovered that the suppression of the variegated phenotype by low light has a clear temporal component: if seedlings are germinated at 25°C under a low irradiance of 5 μmol photons m^{-2} s^{-1} for 7 d and subsequently shifted to growth at 50 μmol photons m^{-2} s^{-1} for 35 d, *im* plants can be exposed to any growth irradiance and will still exhibit an all green phenotype indistinguishable from the wild type (Rosso et al., 2006). This refinement of the low light suppression of variegation suggests that developmental stage has a critical role to play in whether or not the variegated phenotype will develop. In a recent detailed study, Miura et al. (2007) provided strong evidence that leaf variegation in the *var2* mutant of *Arabidopsis* is the result of an imbalance between the biosynthesis and degradation of the D1 protein, the Q_B binding, reaction center polypeptide of PSII,

which transfers electrons to the PQ pool. However, these results still do not explain the variable pattern of sectoring typically observed during the development of a variegated leaf. Since *var2*, like *im*, is the result of a nuclear mutation, theoretically all cells should exhibit defective chloroplasts. Since this is not the case, Miura et al. (2007) conclude that further research is required to elucidate the physiological basis of the observed variegation patterns.

The objective of this study was to ascertain whether there is a physiological explanation for the green-white sectoring observed in variegated mutants of *Arabidopsis*. We hypothesized that the excitation pressure experienced early during leaf development governs the extent of variegation in the *im* mutant of *Arabidopsis*. Thus, changes in temperature should mimic the effects of irradiance on the extent of variegation observed. The development of a nondestructive imaging technique to quantify the kinetics of leaf variegation allowed us to test this hypothesis by examining the interactive effects of growth irradiance, growth temperature, and photoperiod on the extent of variegation during leaf expansion and chloroplast biogenesis.

RESULTS

Consistent with our previous report (Rosso et al., 2006), the cotyledons and the first true leaves of *im* plants germinated and grown at 25°C at an irradiance of 5 μmol photons m^{-2} s^{-1} (25/5) for 7 d under a short-day photoperiod (8/16 h day/night) exhibited an all green phenotype (Figure 2). To determine whether growth irradiance and growth temperature affected the phenotype of the *im* mutant, the *im* seedlings subsequently were shifted to growth at either 50, 150, or 450 μmol photons m^{-2} s^{-1} at 25°C (25/50, 25/150, and 25/450). *im* seedlings exhibited a variegated phenotype upon exposure to growth irradiance greater than 50 μmol photons m^{-2} s^{-1} at 25°C (Figure 2). In parallel, *im* seedlings were shifted to growth at low temperature (12°C) and increasing irradiance (12/50, 12/150, or 12/450).

Leaf development in *im* seedlings was measured microscopically and visually on a daily basis by assessing the number of leaves initiated that were ≥1 mm in length. The wild type and *im* exhibited minimal differences in the rate of leaf initiation (0.030 ± 0.001 leaves/day) throughout growth and development at 25/50 (Figure 3A). After an initial lag period of ~7 d after the shift to increased growth irradiance, the rate of leaf initiation increased in both the wild-type and the *im* seedlings (Figure 3A). Although both genotypes exhibited similar initial rates of leaf initiation at 25/150 (0.04 ± 0.001 leaves/day) and 25/450 (0.07 ± 0.001 leaves/day), the rate of leaf initiation in *im* seedlings deviated significantly from the wild type after ~27 d (Figure 3A). Thus, leaf development in *im* seedlings appeared more sensitive to growth irradiance relative to wild-type seedlings at 25°C.

Leaf expansion was assessed by measuring leaf area in both the wild type and *im* grown at 25°C at 50, 150, and 450 μmol photons m^{-2} s^{-1} (see Supplemental Figure 1 online). Both wild-type (0.13 mm^2/day) and *im* seedlings (0.12 mm^2/day) grown at 25/50 exhibited minimal differences in their exponential growth rates based on leaf area measurements. The exponential rate of leaf expansion appeared to be light saturated at 150 μmol photons m^{-2} s^{-1} (0.20 mm^2/day) in *im* seedlings (see Supplemental Figure 1B online), whereas the exponential rate of leaf expansion increased from 0.22 mm^2/day at 25/150 to 0.28 mm^2/day at 25/450 in wild-type seedlings (see Supplemental Figure 1A online). The time required to reach the mid-log phase of growth at 25°C decreased from ~33 to 35 d at 50 μmol photons m^{-2} s^{-1} to 15 to 17 days at 150 and 450 μmol photons m^{-2} s^{-1} for both wild-type and *im* seedlings (see Supplemental Figure 1A online). As expected, the time required to reach the mid-log phase of growth for both wild-type and *im* seedlings at 12°C increased approximately twofold at an irradiance of either 150 or 450 μmol photons m^{-2} s^{-1} and ~1.2-fold at an irradiance of 50

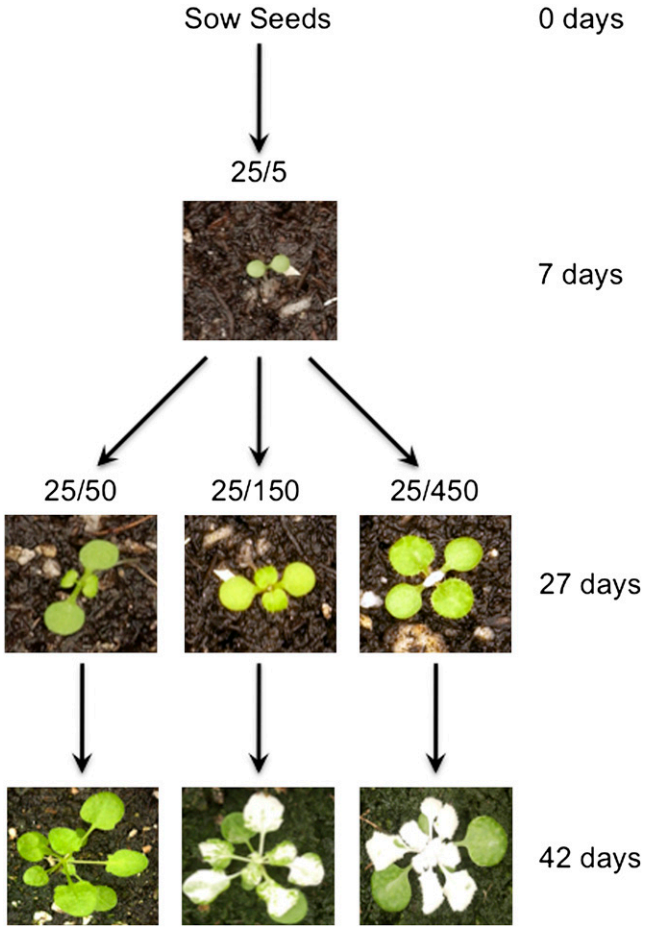

Figure 2. The Experimental Design to Assess the Effects of Light and Temperature on the Development of Variegation in the *im* Mutant of *Arabidopsis*.

Seeds from both the wild type and *im* were germinated and allowed to grow at 25°C under an irradiance of 5 μmol photons m^{-2} s^{-1} (25/5) for 7 d. One group of these seedlings was shifted to either 50 (25/50), 150 (25/150), or 450 (25/450) μmol photons m^{-2} s^{-1} for up to 42 d. In addition, a second group of the same seedlings was shifted to 12°C at an irradiance of 50 (12/50), 150 (12/150), and 450 (12/450) μmol photons m^{-2} s^{-1}. All plants were grown with an 8/16-h day/night cycle. Photographs shown are only of *im* plants.

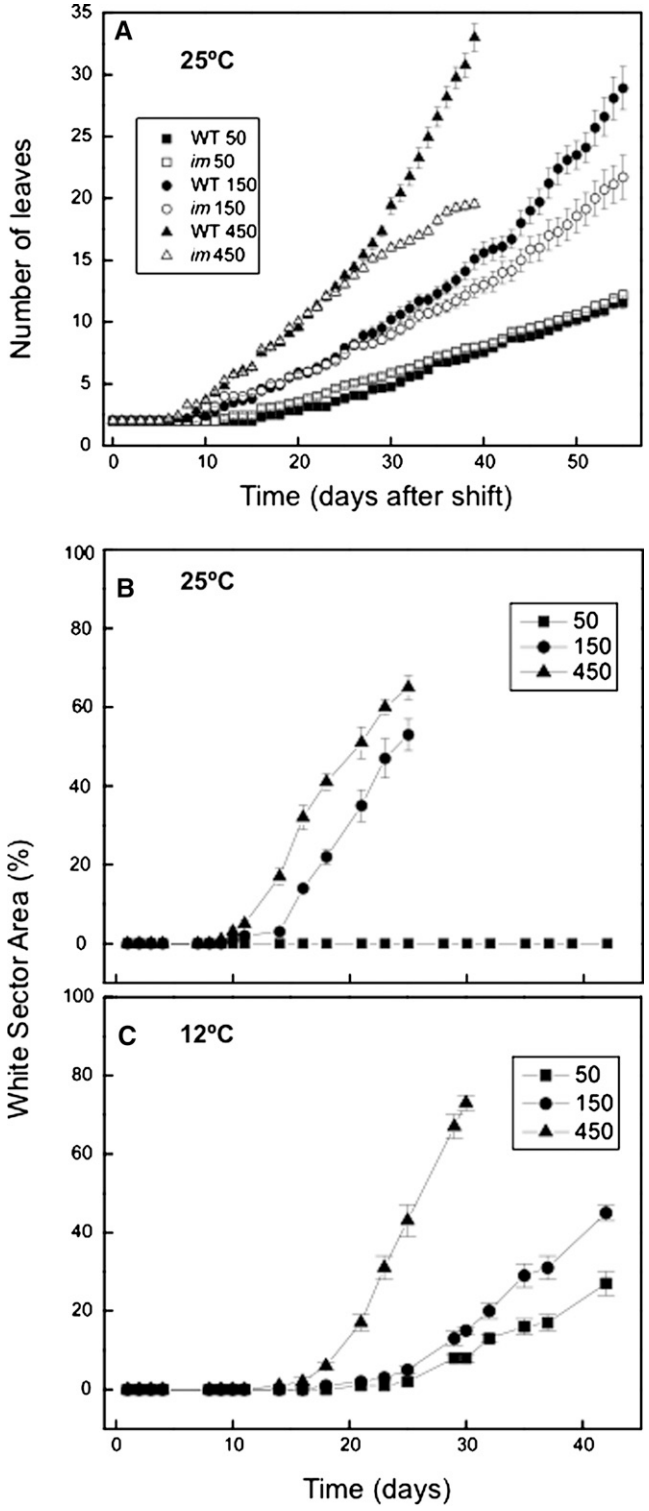

Figure 3. Analysis of Leaf Initiation and Variegation during Seedling Development.

(A) Kinetics of leaf initiation was assessed by counting, on a daily basis, the number of leaf initials that were ≥1 mm in size for both wild-type (closed symbols) and *im* (open symbols) plants. Counting began exactly 7 d after seeding at 5 μmol photons m^{-2} s^{-1} at 25°C to prevent the onset of white sectors in the cotyledons. Both genotypes were grown at 25°C at an irradiance of either 50, 150, or 450 μmol photons m^{-2} s^{-1}. All plants were grown under an 8/16-h day/night cycle.

(B) and **(C)** The kinetics of variegation in *im* seedlings. Variegation was estimated as the percentage of leaf area that was white in *im* plants using the nondestructive method described in Methods. Plants were grown at either 25°C **(B)** or at 12°C **(C)** at an irradiance of either 50, 150, or 450 μmol photons m^{-2} s^{-1}. All plants were grown with an 8/16-h day/night cycle. Data represent the mean ± SE from 10 plants per time point.

μmol photons m^{-2} s^{-1} compared with leaf expansion at 25°C (see Supplemental Figure 1 online).

Effects of Irradiance and Temperature on the Extent of Leaf Variegation

The kinetics for the development of leaf variegation were quantified nondestructively in intact *im* seedlings initially germinated and grown at 25/5 and subsequently shifted to either 25/50, 25/150, or 25/450 by calculating the ratio of the area of white sectors to total leaf area per plant as a function of time. Leaves of *im* seedlings that developed at 25/50 produced no white sectors (Figure 3B, closed squares) and thus exhibited an all green phenotype as previously reported by Rosso et al. (2006). However, after an initial lag of ~15 d, the percentage of leaf white sector areas increased to ~50% at 25 d for seedlings grown at 25/150 (Figure 3B, closed circles). Growth of *im* seedlings at 25/450 not only decreased the initial lag time for the development of white sectors to ~10 d but also increased the extent of variegation to ~65% at 25 d after the shift from 25/5 (Figure 3B, closed triangles).

If excitation pressure controls the variegated phenotype in *im* seedlings, then exposure to low temperature should enhance the development of leaf variegation. In contrast with growth of *im* seedlings at 25°C, *im* seedlings exhibited a variegated phenotype at all irradiances tested during growth at 12°C (Figure 3C). *im* seedlings exhibited 25% variegation when grown at 12°C even at an irradiance of 50 μmol photons m^{-2} s^{-1} for 42 d. Similar to that observed during growth at 25°C, the lag time required to detect leaf variegation decreased with an increase in growth irradiance, and the extent of variegation increased as a function of growth irradiance as measured after 30 d (Figure 3C). As expected, the lag time for the induction of the variegated phenotype increased ~1.5-fold during growth at either 12/150 or 12/450 (Figure 3C) compared with growth at either 25/150 or 25/450 (Figure 3B).

While using intact plants to measure the percentage of white sectors is an appropriate way to investigate the extent of variegation nondestructively, leaves of *Arabidopsis* exhibit overlap as the rosette develops. This would introduce a systematic error in our attempts to quantify the proportion of white versus green sectors in mature plants. To test the accuracy of our nondestructive method, we quantified the extent of variegation using excised leaves, thus eliminating the potential error due to leaf overlap. Figure 4 illustrates the effects of growth irradiance at 25°C (Figure 4A to 4C) and 12°C (Figures 4D to 4F) on the extent

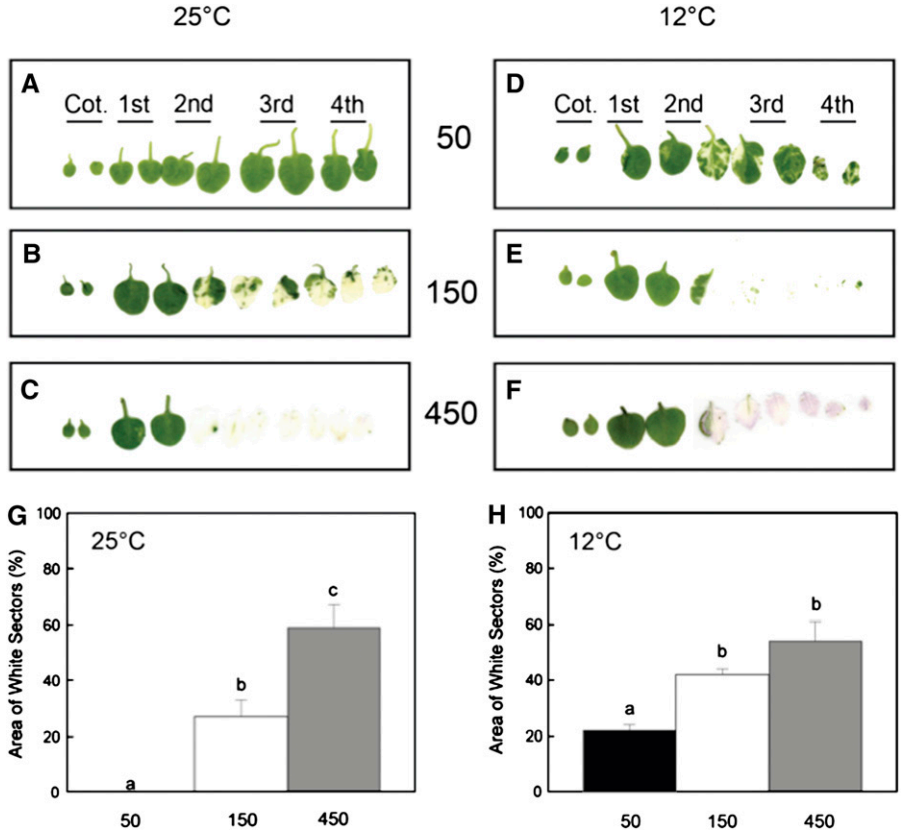

Figure 4. Leaf Phenotype and Quantified Variegation of Excised Leaves.

(A) to **(C)** Leaf scans performed on *im* plants that were grown at 25°C and either 50, 150, or 450 μmol photons m^{-2} s^{-1}. The leaf scans are arranged in consecutive order of development, from the cotyledons (Cot.) to the 4th leaf pair. All plants were grown under an 8/16-h day/night cycle.
(D) to **(F)** Leaf scans were performed as described above except *im* plants were grown at 12°C and either 50, 150, or 450 μmol photons m^{-2} s^{-1}.
(G) and **(H)** Quantification of variegation from the scans for *im* leaves developed at 25°C **(G)** or 12°C **(H)** and either 50, 150, or 450 μmol photons m^{-2} s^{-1}. Variegation was estimated as the percentage of white sectors as described in Methods. Data represent the mean ± SE calculated from two independent experiments with three to six different plants per treatment. Letters represent statistically significant differences between means at the 95% confidence interval.

of variegation in cotyledons (Figure 4, Cot.) and subsequent leaf pairs (1st to 4th) of the rosette. The trends for the effects of irradiance on the extent of variegation for excised leaves developed at either 25°C (Figure 4G) or 12°C (Figure 4H) were comparable to those estimated at the end of each experiment illustrated in Figures 3B and 3C. However, we found that the nondestructive method systematically overestimated the proportion of white to green sectors by 5 to 10% in mature plants compared with the destructive method. We noted with interest that cotyledons (Figures 4A and 4D, Cot.) and the first true leaves (Figures 4A and 4D, 1st) of *im* plants exhibited an all green phenotype irrespective of conditions during growth under an 8-h photoperiod (Figures 4A to 4F).

Our growth kinetic data indicated that low temperature increases the time required to reach mid-log phase of growth in wild-type and *im* plants. However, by comparing plants at the mid-log phase of growth, we were able to assess the interactive effects of growth irradiance and growth temperature on the extent of variegation in *im* seedlings at the same developmental stage. At mid log-phase during growth at 25°C, the proportion of white sectors was 0, 8, and 25% at 50, 150, and 450 μmol photons m^{-2} s^{-1}, respectively. By contrast, at mid-log phase during growth at 12°C, the proportion of white sectors was 20, 40, and 60% at 50, 150, and 450 μmol photons m^{-2} s^{-1}. Thus, when measured at the same developmental stage, *im* seedlings exhibited greater variegation at low temperature than at 25°C irrespective of irradiance. Thus, it appears that the extent of variegation is the result of a complex interaction between growth irradiance and growth temperature.

Effects of Irradiance and Temperature on Excitation Pressure and Photoacclimation

Excitation pressure, measured as 1 – qP, is an estimate of the proportion of closed PSII reaction centers, which reflects the redox state of the PET chain. Consequently, excitation pressure should be sensitive to both irradiance and temperature (Dietz et al., 1985; Hüner et al., 1998, 2003; Wilson et al., 2006). Since

IM is considered to be a plastid terminal oxidase capable of oxidizing the intersystem PQ pool (Joët et al., 2002; Josse et al., 2003, Aluru and Rodermel, 2004; Streb et al., 2005; Stepien and Johnson, 2009), we examined the effects of either changes in measuring irradiance or measuring temperature on excitation pressure in *im* seedlings. The data in Figure 5A illustrate the light response curves for excitation pressure in fully expanded leaves of *im* seedlings grown at 25/50, which results in an all green phenotype. At a measuring temperature of 25°C (closed squares), excitation pressure in *im* seedlings exhibited the expected light saturation response to increasing measuring irradiance and resulted in an apparent quantum requirement, estimated from the initial slope of the light response curve, of 263 μmol photons absorbed to close 50% of the PSII reaction centers. However, lowering the measuring temperature from 25 to 5°C (open squares) significantly increased excitation pressure at any given irradiance, and as a result, the quantum requirement decreased to only 63 μmol photons absorbed to close 50% of PSII reaction centers. The sensitivity of PSII reaction centers to closure increased fourfold by simply decreasing the measuring temperature from 25 to 5°C (Figure 5A). Thus, excitation pressure in *im* seedlings responds to short-term light and temperature changes as expected (Maxwell et al., 1995a) and in a similar fashion to that observed for the wild type.

However, can *im* seedlings photoacclimate in response to increased growth irradiance? If so, then *im* seedlings should respond to increased growth irradiance by decreasing the efficiency of PSII reaction center closure. This can be detected as an increase in the quantum requirement for PSII closure measured as a decrease in the initial slope of the light response curve for excitation pressure. The data in Figure 5B illustrate that the initial slope of the light response curves for excitation pressure in green sectors decreased as the irradiance for growth and development of *im* seedlings increased from 50 to 450 μmol photons m^{-2} s^{-1}. As a consequence, the quantum requirement for PSII closure in green sectors increased with increasing growth irradiance from 298 to 439 to 610 μmol photons absorbed to close 50% of PSII reaction centers in *im* seedlings grown at 25/50, 25/150, and 25/450, respectively. Similar trends were observed for growth of *im* seedlings under increasing irradiance at 12°C (see Supplemental Figure 2 online). Since *im* seedlings decreased their efficiency for PSII closure in response to either high growth irradiance or low growth temperature, we conclude that *im* seedlings photoacclimate to excitation pressure as reported previously for wheat (*Triticum aestivum*), rye (*Secale cereale*), the green algae *C. vulgaris* and *D. tertiolecta*, as well as the cyanobacterium *P. boryanum* (Hüner et al., 2003).

Although excitation pressure may be calculated as either 1-qP (Dietz et al., 1985; Schreiber et al., 1994; Hüner et al., 1998) or 1-qL (Kramer et al., 2004; Baker, 2008), the use of the Heinz-Walz Imaging PAM (see Methods) precludes the ability to calculate qL. However, our previous results (Rosso et al., 2006) indicate that although the absolute values of excitation pressure may vary depending upon whether it is calculated as 1-qP or 1-qL, the trends do not.

Interaction of Photoperiod, Temperature, and Irradiance on Excitation Pressure and Leaf Variegation

Plant development is very sensitive to photoperiod (Bae and Choi, 2008). In our experimental design (Figures 2 and 3), all seedlings were grown under a short-day, 8-h photoperiod to prevent flowering and to ensure that they remained in the vegetative state over the course of our experiments. To assess the potential influence of photoperiod on the extent of variegation, we exposed *im* seedlings to continuous light (CL) under growth conditions of either 25/50, 25/150, or 25/450 (Figure 6). *im* seedlings grown under CL exhibited an increase in variegation at

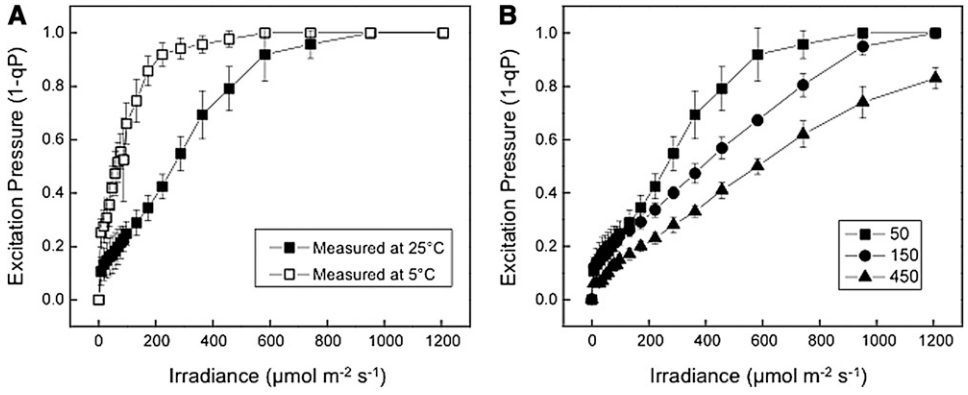

Figure 5. The Effects of Irradiance and Temperature on Excitation Pressure and Photoacclimation in *im*.

(A) The effects of measuring temperature on excitation pressure (1-qP) light response curves for the *im* mutant of *Arabidopsis*. *im* seedlings were grown to mid-log phase at 25°C and 50 μmol photons m^{-2} s^{-1}. Excitation pressure was measured on attached leaves at either 25°C (closed squares) or at 5°C (open circles) with increasing irradiance from 0 to 1200 μmol photons m^{-2} s^{-1}.

(B) The effects of growth irradiance on excitation pressure (1-qP) in attached leaves of *im* seedlings. Plants were grown to mid-log phase at either 25/50, 25/150, or 25/450 and measured at 25°C with increasing irradiance from 0 to 1200 μmol photons m^{-2} s^{-1}. For both **(A)** and **(B)**, plants were grown with an 8/16-h day/night cycle, and attached leaves were measured 4 h into the photoperiod. Data represent the mean ± SE calculated from two independent experiments with three to six different plants per treatment.

25°C as irradiance increased from 50 to 450 μmol photons m^{-2} s^{-1} (Figure 6) similar to that observed for *im* seedlings grown under the short-day photoperiod (Figure 4). However, in contrast with growth under a short-day photoperiod and 50 μmol photons m^{-2} s^{-1}, which induced no variegation (Figures 3B and 4G), *im* seedlings grown under CL at the same irradiance exhibited 30% variegation (Figure 6), which is similar to that observed for *im* seedlings grown at 50 μmol photons m^{-2} s^{-1} but at low temperature (12°C) (Figures 3C and 4H).

The extent of variegation induced by CL also appeared to be a response to increased excitation pressure (Figure 6). At mid-log phase of vegetative growth, *im* seedlings grown under an 8-h photoperiod at 25/50 exhibited the lowest excitation pressure (1-qP = 0.16 ± 0.01), at 25/150 exhibited moderate excitation pressure (1-qP = 0.345 ± 0.01), whereas those grown at 25/450 exhibited the highest excitation pressure (1-qP = 0.500 ± 0.01). Consequently, we observed a strong, positive correlation (R^2 = 0.750) between excitation pressure and the extent of variegation irrespective of whether excitation pressure was modulated by irradiance, low temperature, or by exposure to CL (Figure 7).

In addition to *im*, several other mutants of *Arabidopsis*, such as *spotty*, *var1*, and *var2*, exhibit a variegated phenotype (Aluru et al., 2006; Miura et al., 2007). Consequently, we examined the effects of varying the growth irradiance regime at 25°C for *spotty*, *var1*, and *var2* (Figure 8). The extent and pattern of variegation for *spotty* (Figure 8; see Supplemental Figure 3 online) was very similar to those observed for *im* (Figure 8). Although both *var1* and *var2* also exhibited an increase in the extent of variegation as a function of growth irradiance at 25°C (Figure 8), the patterns of leaf sectoring and the pigmentation of the variegated sectors were distinct from those observed for either *im* or *spotty*. Furthermore, variegation in *var2* appeared to be more sensitive to growth irradiance than either *im*, *spotty*, or *var1* since significant variegation could be detected in the former even at the low growth irradiance of 50 μmol m^{-2} s^{-1} under an 8-h photoperiod (Figure 8; see Supplemental Figure 3 online). Irrespective of the irradiance, growth at 12°C enhanced the extent of variegation in *spotty*, *var1*, and *var2* (see Supplemental Figure 4 online) as was observed for *im* (Figures 3 and 4; see Supplemental Figure 4 online). Since IM cannot compete with P_{700}^+ of PSI for PSII-generated electrons in fully expanded leaves of wild-type seedlings (Rosso et al., 2006), this prompted the question of why the absence of IM leads to variegation under high excitation pressure in *Arabidopsis*.

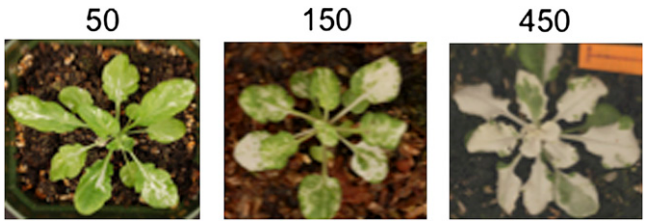

Figure 6. The Effects of Excitation Pressure and CL on Leaf Variegation.

Representative photographs of *im* plants grown at 25°C under CL of either 50, 150, or 450 μmol photons m^{-2} s^{-1}.

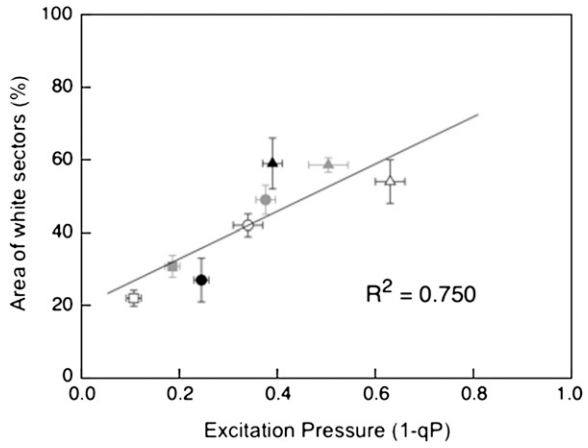

Figure 7. Correlation between Variegation of *im* Seedlings and Excitation Pressure Experienced under Various Growth Conditions.

Variegation was measured as the percentage of white sector area as described in Methods. All plants were germinated and grown for 1 week at 5 μmol photons m^{-2} s^{-1} at 25°C under 8/16-h day/night cycle and were then shifted to different temperature/irradiance conditions for the remainder of the experiment. Temperature/irradiance: closed circles, 25/150; closed triangles 25/450; open squares, 12/50; open circles, 12/150; open triangles, 12/450; closed squares, 25/50 CL; closed circles, 25/150 CL; closed triangles, 25/450 CL. Data represent the mean ± SE with five to six different plants per treatment.

Greening of *im* Cotyledons

Since excitation pressure appeared to regulate the extent of variegation in *im* seedlings (Figure 7), we hypothesized that IM may be important in keeping the PQ pool oxidized early in chloroplast biogenesis during the assembly of the photosynthetic apparatus. To test this hypothesis, both wild-type and *im* knockout seedlings were germinated and grown in the dark prior to exposure to either low or high irradiance at 25°C under CL conditions for 24 h. The greening of cotyledons was used to assess etioplast-to-chloroplast conversion in both the wild type and *im*. Although all wild-type cotyledons exhibited normal greening at either 50 or 150 μmol photons m^{-2} s^{-1} (Figure 9A), 75% of the *im* cotyledons that were subjected to greening at 50 μmol photons m^{-2} s^{-1} exhibited an all green phenotype whereas 25% were variegated (Figures 9A and 9B). By contrast, only 25% of the *im* cotyledons that were subjected to greening at 150 μmol photons m^{-2} s^{-1} exhibited an all green phenotype, whereas 75% were variegated (Figures 9A and 9B). This visual scoring was confirmed by quantifying total chlorophyll per seedling after 24 h greening. Both wild-type (63 ± 11 ng chlorophyll/seedling) and *im* seedlings (64 ± 11 ng chlorophyll/seedling) exhibited similar chlorophyll levels when exposed to greening at 50 μmol photons m^{-2} s^{-1}. By contrast, the chlorophyll content of wild-type etiolated seedlings exposed to greening at 150 μmol photons m^{-2} s^{-1} was 72 ± 6 ng chlorophyll/seedling, whereas greening of *im* etiolated seedlings at the same irradiance resulted in 56% decrease in chlorophyll content (28 ± 5 ng chlorophyll/seedling). Furthermore, even after an extension of the greening time to 72 h at 150 μmol photons m^{-2} s^{-1}, 60% of *im* seedlings

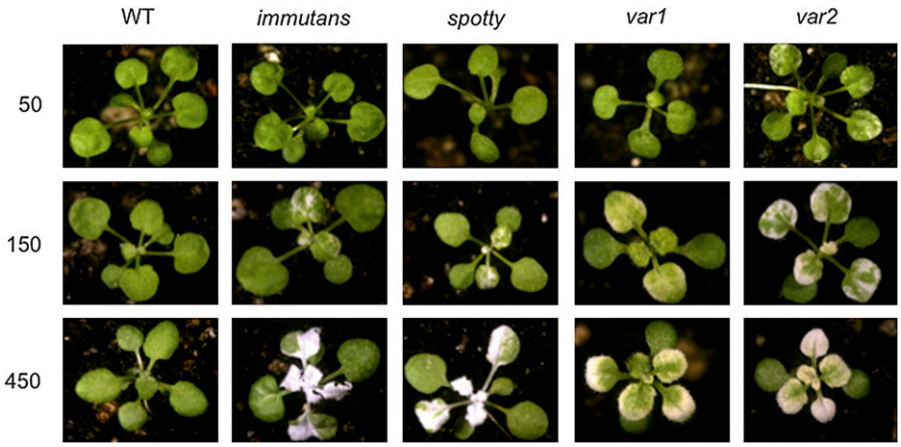

Figure 8. Representative Photographs of Wild-Type, *im*, *spotty*, *var1*, and *var2* Seedlings Grown at 25°C at an Irradiance of Either 50, 150, or 450 μmol Photons m^{-2} s^{-1}.

exhibited an all white phenotype, 32% were variegated, and 8% exhibited an all green phenotype.

Protochlorophyllide oxidoreductase (POR) is the major polypeptide associated with the prolamellar bodies of etioplasts, and its disappearance represents an excellent marker for the conversion of etioplasts to chloroplasts (Biswal et al., 2003; Philippar et al., 2007; Sakamoto et al., 2008). Similarly, Lhcb2, a major polypeptide of PSII light-harvesting pigment protein complex, PsbA, the D1 reaction center polypeptide of PSII, and PsaA/B, the reaction center polypeptide of PSI, were used as markers for the biogenesis of thylakoid membranes (Biswal et al., 2003; Minai et al., 2006). Ribulose-1,5-bisphosphate carboxylase/oxygenase was used as a marker for the development of Calvin cycle in the stroma of the chloroplast. The abundance of POR was comparable in wild-type and *im* etiolated cotyledons (Figure 9C, 0). Furthermore, POR abundance decreased similarly during greening under CL at either 50 or 150 μmol photons m^{-2} s^{-1} such that minimal levels were detected after 24 h of greening in both wild-type and *im* cotyledons (Figure 9C). The kinetics for the disappearance of *PORA* mRNA (Figure 9D) was similar to that for the decrease in POR polypeptide levels during greening of both wild-type and *im* cotyledons irrespective of irradiance. In contrast with *PORA*, *PHYA* expression remained relatively constant throughout the greening process, and no trends in differential *PHYA* expression were observed during greening of wild-type and *im* cotyledons (Figure 9E).

As expected, Lhcb2 polypeptides were not detected in either wild-type or *im* etiolated cotyledons (Figure 9C, 0). The relative abundance of Lhcb2 increased similarly during greening of both genotypes when exposed to CL of 50 μmol photons m^{-2} s^{-1}. Lhcb2 was detected from 6 h after exposure to 50 μmol photons m^{-2} s^{-1} and reached a maximum abundance after 24 h (Figure 9C). Although the kinetics of Lhcb2 accumulation during greening of wild-type cotyledons appeared to occur independently of irradiance, Lhcb2 accumulation during greening of *im* cotyledons appeared to be irradiance dependent. Lhcb2 was detected only after 24 h of greening of *im* cotyledons under CL at 150 μmol photons m^{-2} s^{-1} and was present at reduced levels relative to greening of *im* cotyledons at 25/50 (Figure 9C). In the wild type, PsaB was detectable between 3 and 6 h followed by the detection of PsbA after 6 to 12 h of greening at 150 μmol photons m^{-2} s^{-1}, whereas their appearance was delayed during greening of *im* cotyledons relative to the wild type (see Supplemental Figure 5 online). RbcL was present in etiolated cotyledons, and its abundance increased similarly as a function of greening time in both wild-type and *im* seedlings irrespective of irradiance (Figure 9C).

Differential Changes in PSII Photochemistry during Greening of Cotyledons

The parameter F_v/F_m is a measure of the maximum photochemical efficiency of PSII and can be used as an indicator of the competence of PSII photochemistry and PET (Schreiber et al., 1994; Kramer et al., 2004; Baker, 2008). Upon exposure of etiolated wild-type (closed symbols) and *im* cotyledons (open symbols) to greening under CL at 50 μmol photons m^{-2} s^{-1}, there was an initial lag of ~3 h in F_v/F_m (Figure 10A). Maximum F_v/F_m was attained after 24 h in both the wild-type control (F_v/F_m = 0.760 ± 0.005) and *im* cotyledons (F_v/F_m = 0.658 ± 0.023). Thus, the final F_v/F_m of *im* cotyledons was only ~13% lower than that of wild-type seedlings after 24 h of greening at low light (Figure 10A).

When wild-type etiolated cotyledons were exposed to greening under CL at 150 μmol photons m^{-2} s^{-1}, the F_v/F_m increased to 0.765 ± 0.01 after 24 h of exposure with no initial lag period (Figure 10B, closed symbols). By contrast, *im* etiolated cotyledons exposed to greening still exhibited an initial 3-h lag time after which F_v/F_m increased to a maximum of only 0.471 ± 0.03 after 24 h (Figure 10B, open symbols). Thus, after 24 h of greening at 150 μmol photons m^{-2} s^{-1}, F_v/F_m of *im* cotyledons was 38% lower than that of wild-type controls. The apparent inhibition of PSII photochemistry during greening at the higher irradiance in *im* cotyledons compared with the wild type (Figure 10B) is consistent with the inhibition of chlorophyll accumulation in *im* cotyledons (Figures 9A and 9B).

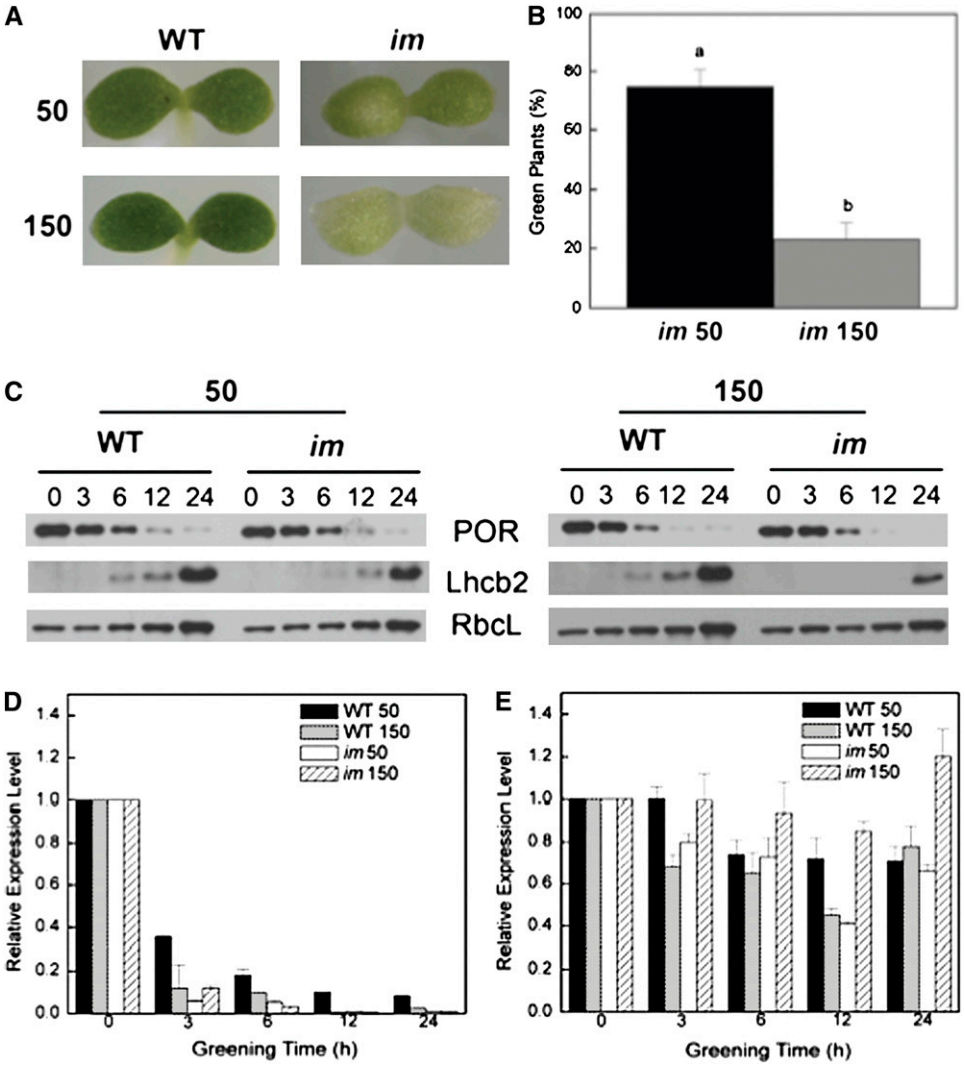

Figure 9. The Effects of Irradiance on Chloroplast Development.

(A) Representative photographs showing cotyledons of wild-type and *im* plants germinated at 25°C and either 50 or 150 μmol photons m^{-2} s^{-1}.
(B) The effect of growth irradiance on the proportion of green seedlings in *im*. 625 seedlings (25 per agar plate) were germinated in the dark for a period of 5 d and subsequently exposed to continuous irradiance of either 50 or 150 μmol photons $m-2$ s^{-1} for 24 h at 25°C. The number of green versus either variegated or white cotyledons was scored visually. Letters represent statistically significant differences between means at the 95% confidence interval. Data represent the means ± SE.
(C) Accumulation of chloroplast polypeptides in wild-type and *im* cotyledons as a function of time (h) during greening. Seeds were germinated in the dark for 5 d and subsequently exposed to CL of either 50 or 150 μmol photons m^{-2} s^{-1} for up to 24 h at 25°C. SDS-PAGE was performed using equal amounts of protein per lane. Immunoblots were probed with polyclonal antibodies raised against POR, Lhcb2, and RbcL as described in Methods.
(D) Relative expression level of *PORA* mRNA during greening of dark-grown wild-type and *im* cotyledons at either 50 or 150 μmol photons m^{-2} s^{-1} using qRT-PCR. The relative expression levels of mRNA in three replicate samples were normalized to *Actin2*, which served as the endogenous control, and were standardized to a calibrator sample consisting of mRNA from dark-grown wild-type seedlings (0 h) at both 50 and 150 μmol photons m^{-2} s^{-1}, at 25°C. Data represent the means ± SE.
(E) Relative expression level of *PHYA* mRNA during greening of dark-grown wild-type and *im* cotyledons at either 50 or 150 μmol photons m^{-2} s^{-1} using qRT-PCR. All conditions are identical to those described in **(D)**. Data represent the means ± SE.

Concomitantly, excitation pressure (1-qP) was measured in both wild-type and *im* etiolated cotyledons exposed to greening under CL at 50 μmol photons m^{-2} s^{-1}. After 3 h of exposure to CL, 80 to 90% of the PSII reaction centers in wild-type (1-qP = 0.834 ± 0.07) and *im* cotyledons (1-qP = 0.908 ± 0.020) were still closed (Figure 10C). However, 1-qP decreased dramatically between 3 and 6 h of greening and remained relatively constant for the duration of the greening period such that after 24 h, wild-type cotyledons exhibited a 1-qP of 0.227 ± 0.020 and the mutant a 1-qP value of 0.160 ± 0.020 (Figure 10C). This indicates

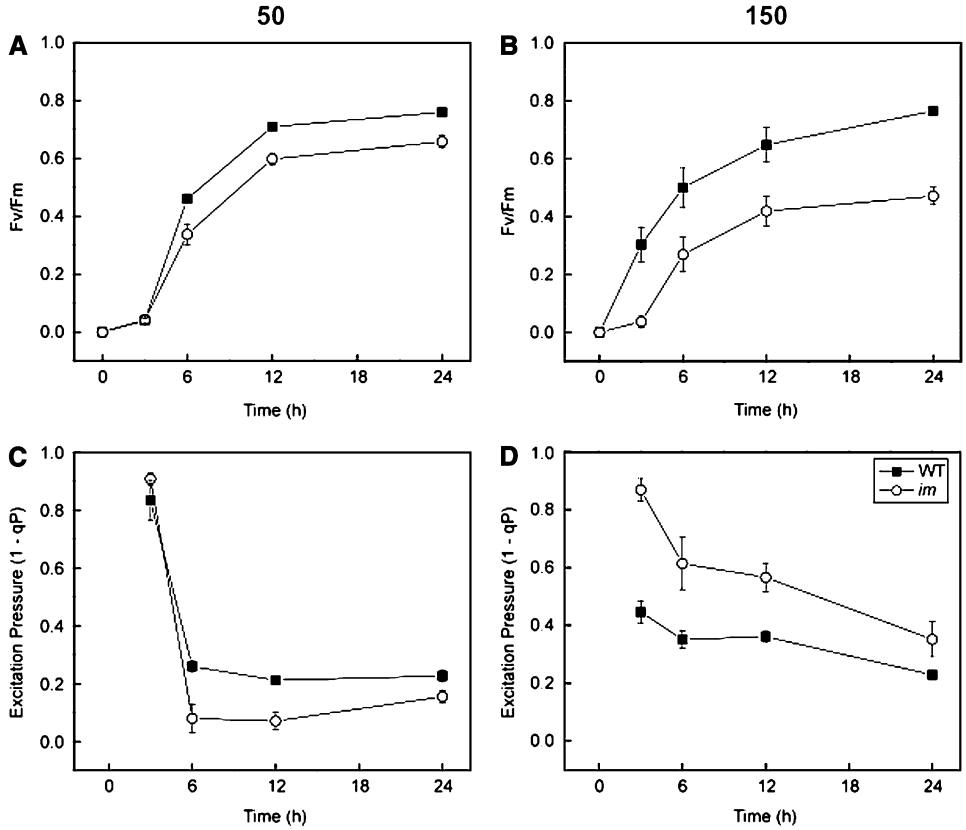

Figure 10. The Development of PSII Photochemistry in the Wild Type and *im*.

(A) and **(B)** Development of maximum PSII photochemical efficiency (F_v/F_m) during greening of etiolated wild-type and *im* cotyledons at 25°C under an irradiance of either 50 **(A)** or 150 **(B)** μmol photons m^{-2} s^{-1}. Data represent mean ± SE of 5 to 11 different seedlings per time point.
(C) and **(D)** The effect of greening time on excitation pressure (1-qP) in etiolated wild-type and *im* cotyledons. For each time point, 250 seeds among 10 agar plates were germinated in the dark for 5 d and subsequently exposed to CL of either 50 or 150 μmol photons m^{-2} s^{-1} for up to 24 h at 25°C. All seedlings were dark adapted for 20 min prior to measurement of F_v/F_m and 1-qP. Data represent the mean ± SE from 5 to 11 different seedlings per time point.

that PSII reaction centers opened rapidly in the first 6 h of greening at low irradiance for both wild-type and *im* cotyledons.

In contrast with greening at 50 μmol photons m^{-2} s^{-1}, excitation pressure was significantly lower after 3 h of greening at 150 μmol photons m^{-2} s^{-1} in wild-type (1-qP = 0.446 ± 0.040) than *im* cotyledons (1-qP = 0.869 ± 0.040) (Figure 10D). This trend persisted throughout the 24-h greening process under CL at 150 μmol photons m^{-2} s^{-1}, which indicates that a greater proportion of PSII reaction centers remained closed in *im* than wild-type cotyledons during greening under CL at 150 μmol photons m^{-2} s^{-1}. Since *im* cotyledons cannot synthesize carotenoids involved in the xanthophyll cycle (Wetzel et al., 1994), nonphotochemical quenching (qN) capacity did not change during the 24-h greening period, whereas wild-type cotyledons exhibited a 1.5-fold increase in qN after 12 h of greening. Thus, the differential sensitivity of greening to irradiance in *im* compared with wild-type cotyledons was associated with the maintenance of a higher excitation pressure in *im* seedlings especially during the first 12 h of greening.

Effects of a Short Pulse of High Light on Greening in Cotyledons

To test whether the apparent differential excitation pressure observed during the first 12 h of greening in the wild type versus *im* cotyledons (Figure 10D) affects chloroplast biogenesis, etiolated cotyledons of wild-type and *im* cotyledons were subjected to a single, 60-min pulse of high excitation pressure created by high light exposure (HL; 700 μmol photons m^{-2} s^{-1}) at various times during early chloroplast biogenesis and subsequently shifted back to a continuous low-light greening regime (LL; 15 μmol photons m^{-2} s^{-1}). If uninterrupted, this treatment should result in a comparable all green phenotype in the wild type as well as *im* . This HL irradiance was chosen because, based on the data presented in Figure 5B (closed squares), exposure to 700 μmol photons m^{-2} s^{-1} would be sufficient to create maximum excitation pressure (1-qP = 1.0) in low-light-grown *im* seedlings. Figure 11 (control) confirmed that the chlorophyll content of wild-type (Figure 11, black bar) and *im* cotyledons (Figure 11, white bar) subjected to greening for 24 h under the continuous LL were

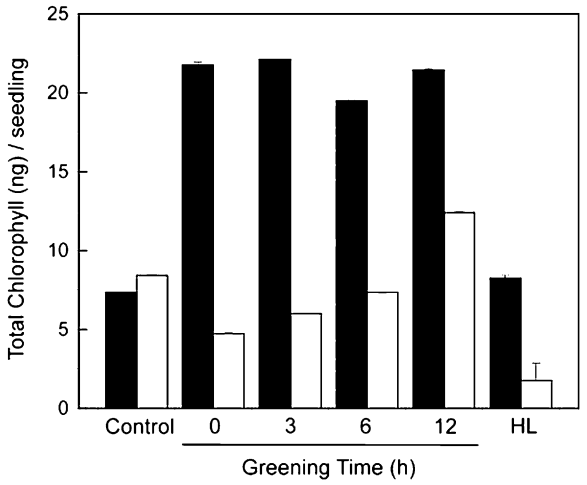

Figure 11. The Effects of a HL Pulse on the Greening in Wild-Type and *im* Cotyledons.

Seeds of the wild type and *im* were germinated on agar plates and grown in the dark as described for Figure 9. Etiolated cotyledons were then shifted to low light (LL; 15 μmol photons m^{-2} s^{-1}) at 25°C to initiate greening. The extent of greening was quantified as total chlorophyll per seedling in the wild type (closed bars) and *im* (open bars). Control etiolated cotyledons were exposed to greening under continuous LL for 24 h. In addition, etiolated wild-type and *im* cotyledons were exposed to a 23 h of greening at LL, which was interrupted by a 60 min of exposure to HL (700 μmol photons m^{-2} s^{-1}) either prior to exposure to greening at LL (0 greening time) or after 3, 6, or 12 h of greening under continuous LL. After the 60 min exposure to HL, cotyledons were transferred back to continuous LL to complete the 24 h of greening. After 24 h of greening, the total chlorophyll accumulated per seedling was determined. The data represent the means ± SD of three replicate chlorophyll measurements within a single experiment. The number of seedlings used per treatment ranged between 80 and 150.

indeed comparable, indicating normal chloroplast biogenesis in both genotypes.

However, exposure of wild-type etiolated cotyledons to a single, 60-min pulse of HL stimulated chlorophyll accumulation threefold to fourfold relative to controls during subsequent greening at LL regardless of time at which this pulse of HL was imposed within the first 12 h of greening. In contrast with the wild type, etiolated *im* cotyledons immediately exposed to 60 min of HL (Figure 11, 0 greening time, white bar) prior to subsequent greening for an additional 23 h at LL, exhibited a 50% reduction in chlorophyll content relative to controls. Chlorophyll accumulation during greening of *im* cotyledons was also inhibited relative to controls when the HL pulse was imposed at either 3 or 6 h of greening at LL. However, the inhibition of chlorophyll accumulation in *im* cotyledons appeared to be less severe at either 3 or 6 h than at the 0 h greening time (Figure 11, white bars). Only after 12 h of greening at LL did the imposition of a 60 min pulse of HL stimulate chlorophyll accumulation by ~60% in *im* cotyledons. As expected, the trends for chlorophyll accumulation using either a 30- or 90-min pulse of HL were similar to that shown in Figure 11 except that the extent of the inhibition during greening of *im* cotyledons was lower using a 30-min pulse but greater with the 90-min pulse during the first 6 h of greening relative to the effects of the 60-min pulse of HL (see Supplemental Figure 6 online).

However, irrespective of the duration of the HL pulse, *im* cotyledons exhibited a 53 to 76% stimulation in chlorophyll accumulation relative to controls when the HL pulse was imposed at 12 h of greening (see Supplemental Figure 6 online). By contrast, the HL pulse stimulated chlorophyll accumulation during the greening of wild-type cotyledons under LL irrespective of duration of the HL pulse (see Supplemental Figure 6 online). Although exposure of wild-type cotyledons to greening under continuous HL for 24 h resulted in chlorophyll levels comparable to those exposed to greening for 24 h at LL (Figure 11, HL, black bar), as expected, exposure of *im* cotyledons to the same continuous HL greening regime for 24 h inhibited chlorophyll accumulation by fourfold to fivefold (Figure 11, HL, white bar) such that these seedlings exhibited a white phenotype. Thus, chloroplast biogenesis in *im* seedlings appeared to be most sensitive to a brief HL exposure during the first 6 h of greening.

Effects of Greening on *IM* and *AOX1a* Expression

If IM plays an important role as a plastid terminal oxidase to keep the PQ pool oxidized during early biogenesis and assembly of the photochemical apparatus of *Arabidopsis*, we hypothesized that *IM* should be transiently expressed. Maximum expression should be induced rapidly during the onset of greening of wild-type *Arabidopsis* followed by a subsequent decrease in expression to constitutive levels after completion of the biogenesis and assembly of the photosynthetic apparatus. In addition, exposure to increased irradiance during greening should significantly enhance the transient expression levels of *IM*. The results for real-time quantitative RT-PCR (qRT-PCR) for *IM* expression in the wild type is illustrated in Figure 12A. In contrast with our hypothesis, the results show that the relative expression of *IM* increased gradually during greening of the wild type under CL at either 50 or 150 μmol photons m^{-2} s^{-1}. Furthermore, the relative expression levels of *IM* during greening of the wild type at 150 μmol photons m^{-2} s^{-1} tended to be lower than that observed for greening at 50 μmol photons m^{-2} s^{-1}.

AOX expression has been shown to be an excellent marker for assessing redox energy imbalances in mitochondria (Vanlerberghe and McIntosh, 1997; Maxwell et al., 1999; Arnholdt-Schmitt et al., 2006; Noctor et al., 2007; McDonald, 2008). In contrast with *IM*, the relative expression of mitochondrial *AOX1a* did exhibit a transient stimulation of expression in the wild type but only when exposed to greening at 150 μmol photons m^{-2} s^{-1} (Figure 12B). After 6 h of greening at 150 μmol photons m^{-2} s^{-1}, the relative *AOX1a* expression levels increased ~3.5-fold and subsequently returned to control levels (Figure 12B, 0) after 24 h of greening. However, greening of wild-type etiolated cotyledons at 50 μmol photons m^{-2} s^{-1} induced minimal changes in *AOX1a* expression compared with controls (Figure 11B, closed bars). Similar to the wild type, *im* etiolated cotyledons exposed to greening at 150 μmol photons m^{-2} s^{-1} also exhibited a 3.5-fold stimulation in the relative expression of *AOX1a* after 6 h relative to controls (Figure 12B, 0). However, the relative level of *AOX1a* expression remained at approximately

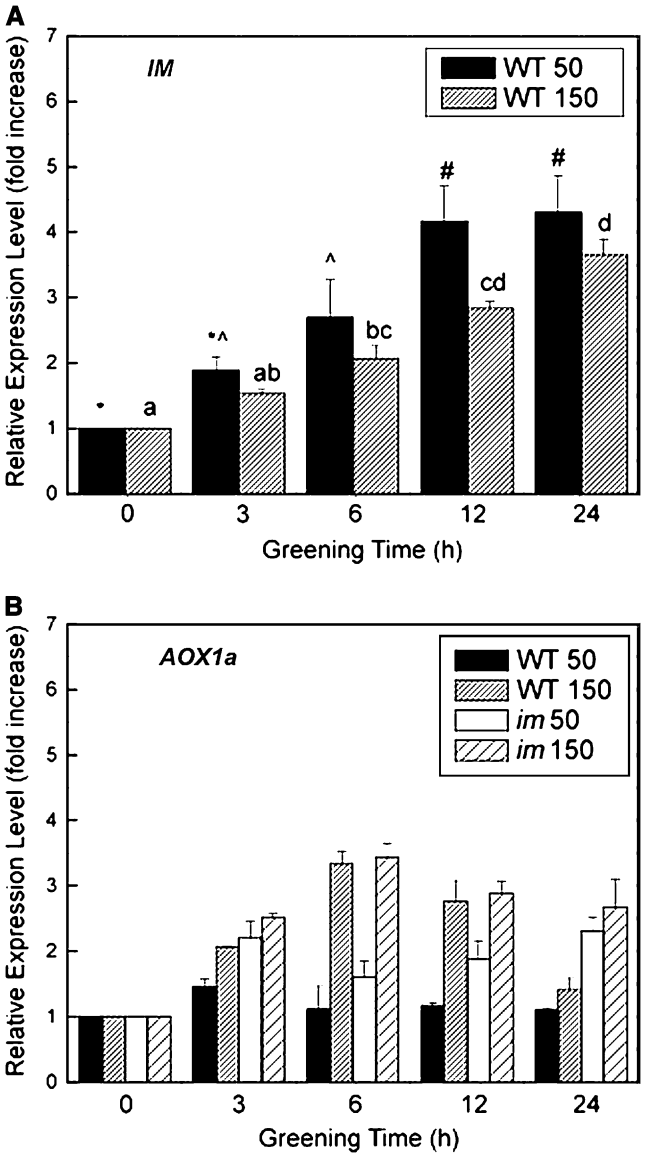

Figure 12. The Effect of Greening on the Relative Expression Levels of *IM* and *AOX1a*.

Seeds of both wild-type and *im* seeds were germinated in the dark for 5 d and subsequently exposed to CL of either 50 or 150 μmol photons m^{-2} s^{-1} for up to 24 h at 25°C. Relative expression levels of *IM* **(A)** and *AOX1a* **(B)** were quantified by qRT-PCR as described in Methods. Data represent the means ± SE of three replicate measurements.

threefold even after 24 h in *im* cotyledons. Even exposure of *im* etiolated cotyledons to greening at 50 μmol photons m^{-2} s^{-1} (Figure 12B, open bars) stimulated the relative expression levels of *AOX1a* by twofold in *im* cotyledons, which remained relatively constant throughout the 24-h greening period. Thus, in contrast with the wild type, the stimulation of *AOX1a* expression in *im* cotyledons persisted throughout the greening period consistent with the proposed role of *AOX1a* in sensing mitochondrial redox imbalance (Giraud et al., 2008).

DISCUSSION

To elucidate the physiological basis for variegation in *im* seedlings, we established an in vivo, nondestructive assay to quantify the extent of variegation as a function of developmental time (Figures 3 and 4). We showed that both the rate of development of the variegated phenotype as well as the overall extent of variegation in *im* seedlings were strongly dependent upon growth irradiance with no variegation detected at a growth irradiance of 50 μmol photons m^{-2} s^{-1} at 25°C and an 8-h photoperiod (Figures 3B and 4A). However, our results clearly indicate that the expression of the variegated phenotype cannot be explained as a simple irradiance effect since growth at the same low irradiance combined with low temperature (12°C) (Figures 3C, 4D, and 4H) resulted in a significant increase in variegation of *im* seedlings.

As a consequence, the development of variegation in *im* seedlings appears to be a complex interaction of irradiance and temperature. We show that the extent of variegation in *im* seedlings is not caused by irradiance and temperature per se, but rather, is governed by excitation pressure which reflects the redox state of the PQ pool of the PET chain (Figure 1). This conclusion is supported by the results of Figure 7, which illustrate a strong, positive correlation between excitation pressure and the extent of variegation regardless of how the excitation pressure was generated. Light initially trapped and transformed through extremely fast, temperature-insensitive photochemistry (in the femtosecond [10^{-15} s] to nanosecond [10^{-9} s] time scale) represents the ultimate form of energy used through much slower, temperature-dependent biochemical processes (ms [10^{-3} s] to s to h time scales) to maintain cellular homeostasis, growth, and development in all photoautotrophs. Thus, imbalances between photochemistry and redox biochemistry result in modulation of the redox state of the PQ pool of PET (Figure 1) as well as the redox state of the ubiquinone pool of mitochondria (Figure 12B), indicating that information regarding energy imbalance is transferred between chloroplasts and mitochondria (Noctor et al., 2007; Aluru et al., 2009). Furthermore, we conclude that variegation governed by the redox state of the PET chain is not restricted to *im*, but rather, also appears to govern variegation in *spotty*, *var1*, and *var2* (Figure 8; see Supplemental Figure 4 online). A common feature of all the mutants tested is that the mutations affect components of the PET chain. *im* and *spotty* are knockout mutants of IM/PTOX, a plastid terminal oxidase of the thylakoid membrane that uses PQH_2 as an electron donor. *var1* and *var2* are genes encoding *FtsH5* and *FtsH2*, respectively, that appear to be involved in PSII photodamage and repair (Aluru et al., 2006; Miura et al., 2007).

Chloroplast biogenesis and the development of a functional photosynthetic apparatus is part of a complex photomorphogenic process in plants. Light has two important roles in this developmental process. First, light quality provides the necessary information for the initiation of photomorphogenesis and plant growth through an integrated network of photoreceptor-mediated signal transduction pathways involving phytochromes (Rockwell et al., 2006; Bae and Choi, 2008), cryptochromes (Li and Yang, 2007; Ruckle et al., 2007), and phototropins (Christie, 2007) as well as a new nonphotoreceptor signal transduction

pathway involving the flavoprotein HAL (Sun et al., 2009). Our results indicate that irradiance and photoperiod influence the extent of variegation in *Arabidopsis*. Since photoreceptors respond to light and photoperiod, can the control of variegation through photoreceptors account for the variable extent of variegation reported here for *im*, *spotty*, *var1*, and *var2*?

In contrast with light and photoperiod, there is no evidence that photoreceptors respond to temperature. Since low temperature mimics the effects of irradiance on the extent of variegation, we conclude that the extent of variegation observed cannot be explained by the action of photoreceptors, such as phytochrome or cryptochrome. Furthermore, the induction of variegation under CL (Figures 6 and 11) can be explained on the basis that the absence of an 8-h photoperiod precludes the possibility for the dark relaxation of excitation pressure by respiratory metabolism in the absence of photosynthesis. Thus, excitation pressure is created by feedback inhibition of PET induced by the accumulation of photosynthetic end products under CL conditions.

The second role for light in plant photomorphogenesis is as the energy source for growth and development. The light trapped by the pigments of the photosystems is initially transformed through extremely fast, temperature-insensitive, photophysical, and photochemical processes. The biogenesis and assembly of PSI and PSII requires tight coordination between the de novo synthesis of chlorophyll and other pigments, lipids as well as chloroplast and nuclear-encoded proteins (Tobin and Silverthorne, 1985; Biswal et al., 2003; Eberhard et al., 2008; Sakamoto et al., 2008). Thus, this raises an important developmental question as to how a photoautotroph mitigates the potential damaging effects of photooxidation during the biogenesis and assembly of its photosystems prior to the establishment of a fully functional photosynthetic apparatus. Important photoprotective mechanisms during chloroplast biogenesis include transient stimulation of nonphotochemical dissipation of excess energy through the xanthophyll cycle (Murchie et al., 2009) as shown during early greening in barley (*Hordeum vulgare*; Krol et al., 1999) as well as the induction of myriad plant oxidative stress genes including *AOX* (Aluru et al., 2009).

Since *im* seedlings are unable to biosynthesize photoprotective carotenoids involved in the xanthophyll cycle (Wetzel et al., 1994) and thus cannot modulate nonphotochemical quenching, we hypothesized that IM may play an important role in photoprotection from photooxidation during early chloroplast biogenesis and assembly of the photosynthetic apparatus prior to the establishment of full photosynthetic competence. The following data are consistent with this hypothesis. First, although greening at low irradiance indicated minimal differences in chloroplast biogenesis based on the disappearance of PORA and the appearance of Lhcb2 in the wild type and *im* (Figure 9C), the accumulation of Lhcb2, PsaB, and PsbA were delayed and the relative abundance of these thylakoid proteins was reduced in *im* cotyledons relative to the wild type during greening at 150 μmol photons m^{-2} s^{-1} (Figure 9C; see Supplemental Figure 5 online). Furthermore, the observed kinetics for the disappearance of PORA and the appearance of PsaB, PsbA, and and Lhcb2 during the greening of wild-type *Arabidopsis* cotyledons are consistent with those published for chloroplast biogenesis in other photoautotrophs (Krol et al., 1987; Biswal et al., 2003; Philippar et al., 2007; Sakamoto et al., 2008).

Second, although the development of maximum PSII photochemical efficiency (F_v/F_m) was stimulated by greening at 150 μmol photons m^{-2} s^{-1} in wild-type cotyledons (cf. Figures 10B and 10A, closed symbols), greening at this higher irradiance impaired the development of PSII photochemistry in *im* cotyledons (cf. Figures 10B and 10A, open symbols). These functional data are consistent with the biochemical data indicating a delayed appearance of both PSII and PSI reaction centers during greening of *im* compared with the wild type (see Supplemental Figure 5 online).

Third, although the kinetics and the extent of the decrease in excitation pressure were comparable for *im* and wild-type cotyledons during greening at 25/50 (Figure 10C), excitation pressure after 3 h of greening at 25/150 was twofold higher in *im* (0.86) than wild-type cotyledons (0.45) (Figure 10D). However, this difference in excitation pressure between *im* and wild-type cotyledons gradually decreased as a function of greening time such that after 24 h, the difference in excitation pressure between *im* and wild-type cotyledons was only 30%. This indicates that *im* seedlings have a greater propensity to accumulate closed PSII reaction centers than wild-type seedlings especially during the early stages of greening.

Finally, the sensitivity of chloroplast biogenesis in *im* seedlings to a pulse of high excitation pressure was greatest between 0 and 6 h of greening (Figure 11; see Supplemental Figure 6 online). Only after 12 h of greening did the imposition of a pulse of high excitation pressure no longer inhibit chlorophyll accumulation relative to the control. In contrast with *im*, the imposition of the same pulse of high excitation pressure during greening of wild-type cotyledons stimulated chloroplast biogenesis regardless of the time during wild-type greening at which the pulse of high excitation pressure was imposed (Figure 11; see Supplemental Figure 6 online). Since the major difference in the complement of the redox components of the photosynthetic electron chain between wild-type and *im* seedlings is the absence of IM in the latter (Rosso et al., 2006), we conclude that IM has a important role in photoprotection from photooxidation by lowering the excitation pressure during the initial early stages of chloroplast biogenesis in *Arabidopsis*. This photoprotective requirement for the presence of IM is developmentally dependent and becomes minimal in mature chloroplasts of *Arabidopsis* with a functional photosynthetic apparatus. However, we do not wish to imply that photoprotection through IM as a plastoquinol oxidase is the only mechanism induced during normal chloroplast biogenesis in *Arabidopsis*. The role of IM as a plastoquinol oxidase must be integrated over time with nonphotochemical quenching (Krol et al., 1999; Falkowski and Chen, 2003; Murchie et al., 2009), and the induction of antioxidant stress genes to prevent photooxidation during chloroplast biogenesis (Aluru et al., 2009).

We note with interest that, although the levels of expression of *IM* increase gradually as a function of greening time in wild-type cotyledons, there are minimal differences in expression levels during greening at either 25/50 or 25/150 (Figure 11A). Thus, *IM* expression is not sensitive to excitation pressure. In fact, the differences in excitation pressure during greening at 25/150 between *im* and wild-type cotyledons appear to be inversely

related to the degree of stimulation of *IM* expression. Clearly, the putative role for IM in photoprotection by modulating excitation pressure during chloroplast biogenesis does not require maximal expression of *IM*. Constitutive levels of IM must be sufficient to keep the PQ pool oxidized during the first 6 h of greening.

Photostasis, that is, photoautotrophic energy balance, involves communication between chloroplasts and mitochondria through the integration of light-dependent, photosynthetic redox reactions with the light-independent respiratory redox reactions. These two redox compartments are linked metabolically through the complex C- and N-metabolic networks. IM exhibits 37% sequence identity to mitochondrial AOX (Wu et al., 1999). Plant *AOX* expression is both developmentally regulated and stimulated by myriad abiotic stresses (Vanlerberghe and McIntosh., 1997; Arnholdt-Schmitt et al., 2006; Clifton et al., 2006; Umbach et al., 2006; McDonald, 2008). In contrast with *IM*, we show that *AOX1a* expression is sensitive to excitation pressure during greening of wild-type and *im* cotyledons (Figure 12B). Although minimal stimulation of *AOX1a* was detected over the course of greening of the wild type at 25/50, 6 h of greening of the wild type at 25/150 induced a transient threefold stimulation of *AOX1a* expression, which returned to control levels upon completion of chloroplast biogenesis after 24 h of greening. By contrast, greening of *im* at 25/50 stimulated *AOX1a* expression approximately twofold, whereas greening at 25/150 stimulated *AOX1a* expression threefold (Figure 12B). Furthermore, this stimulation was not transient during greening of *im* cotyledons but remained high even after chloroplast biogenesis was completed after 24 h. The sensitivity of *AOX1a* to excitation pressure illustrates the important interplay between chloroplast and mitochondrial energy metabolism.

In summary, we report that IM is necessary but not sufficient to account for the variegated phenotype in *im* plants of *Arabidopsis*. We show that chloroplast energy imbalance as detected by increased excitation pressure through modulation of the redox state of the PQ pool governs variegation in *im*, *spotty*, *var1*, and *var2* seedlings. This is consistent with the model proposed by Rodermel and coworkers (Wu et al., 1999; Aluru et al., 2001, 2006, 2009; Aluru and Rodermel, 2004) for *im* seedlings as well as variegation in the *ghost* mutant of tomato (*Solanum lycopersicum*; Barr et al., 2004; Yu et al., 2007) whereby the presence of white sectors are due to chloroplast photooxidation. We agree with Miura et al. (2007) and Eckardt (2007) that variegation in *Arabidopsis* is a consequence of balance. However, the notion of an imbalance between D1 protein synthesis and degradation as suggested by Miura et al. (2007) fails to account for the heterogeneity in chloroplast development evident by the presence of white and green sectors in the *var2* mutant of *Arabidopsis*. We suggest that photosynthetic redox energy imbalance rather than D1 protein turnover governs the extent of variegation in *Arabidopsis* as indicated by modulation of excitation pressure in the chloroplast (Figures 7 and 11; see Supplemental Figure 5 online).

In our opinion, this provides the basis for a simple explanation for the variability not only in the extent but also in the exquisite patterns of variegation observed for *im*, *spotty*, *var1*, and *var2*. Leaf angle relative to incident light, leaf position relative to its nearest neighbors, leaf morphology, and leaf anatomy all dramatically attenuate light capture and light propagation within a mature leaf. This results in a very heterogeneous distribution of light and, thus, gradients of photosynthetic activity within a leaf (Vogelmann et al., 1996). It seems reasonable to suggest that, for the same reasons, internal light will be attenuated during the emergence of cotyledons as well as during leaf initiation and expansion creating a heterogeneous distribution of excitation pressures internally that will affect heterogeneity in chloroplast biogenesis. Thus, green sectors observed in leaves of the variegated seedlings arise because chloroplasts present in those cells develop under sufficiently low excitation pressure (1-qP $\leq$ 0.2; Figure 10C) during early chloroplast biogenesis such that the cellular antioxidant capacity and/or nonphotochemical quenching capacity is sufficient to protect against chloroplast photooxidation. Thus, under these conditions, chloroplast biogenesis in the first 12 h is able to proceed normally and leaf sectors will appear green. By contrast, the combination of either high irradiance at moderate temperature or moderate irradiance at low temperature will induce a variegated phenotype because the cellular antioxidant capacity and/or the nonphotochemical quenching capacity is insufficient to counteract the production of ROS during biogenesis of the photosynthetic apparatus under these high excitation pressure conditions (1-qP $\geq$ 0.4; Figures 10D and 11) and protect the developing chloroplast against photooxidation. Thus, in our opinion, regulation of leaf variegation by photosynthetic redox imbalance can account for the variable sectoring patterns as well as the variable extent of white sectors typically observed during leaf variegation in *im*, *spotty*, *var1*, and *var2*.

METHODS

Growth Conditions

Seeds of *Arabidopsis thaliana* (ecotype Columbia) wild type and the variegated mutants *im* (CS3157; AT4G22260), *var1* (CS271; AT5G42270), and *var2* (CS271; AT2G30950) were obtained from the ABRC (Columbus, OH), and *spotty* was generated as described previously (Wetzel et al., 1994). All seeds were germinated and grown under controlled environment conditions at 25°C with a photosynthetic photon flux density of 5 μmol photons m^{-2} s^{-1} for 1 week. Plants were thinned to one plant per pot and grown at either 25 or 12°C with increasing irradiance of either 50, 150, or 450 μmol photons m^{-2} s^{-1}. All plants were grown with an 8/16-h day/night cycle to prevent the induction of flowering.

For the experiments that monitored the greening of cotyledons, wild-type and *im* seeds were sterilized with 20% (v/v) bleach and 0.05% (v/v) Tween 20 and placed on Petri plates containing 0.5$\times$ Murashige and Skoog basal salt mixture, pH 5.7, with 0.8% (w/v) agar (McCourt and Keith, 1998), with 25 seeds per plate. The plates were placed in the dark at 4°C for 3 d to ensure maximum, synchronized germination. Seeds were then removed from the cold treatment to 25°C but remained in darkness for an additional 5 d. After this dark period, seeds were placed under CL at either 50 or 150 μmol photons m^{-2} s^{-1} for a period of 24 h at 25°C.

Determination of Growth Rate

Growth of both wild-type and *im* plants was measured by two methods. In the first method, leaf initials were observed under a dissecting microscope (Leica Wild M3B) and measured daily. Positive identification of leaf initials was standardized by counting only those leaf initials that were $\geq$1 mm. Second, growth of *Arabidopsis* was also measured by measuring leaf area as a function of time. Leaf area was measured using a dissecting

microscope (Leica Wild M3B) at 4, 10, and ×40 magnification attached to a CCD camera. Digital photos were taken, and leaf area was analyzed using imaging analysis software (Northern Eclipse Image Analysis Software 7.0; Empix Imaging). Leaf area was measured by tracing and measuring the area of each leaf per plant. The image analysis software was calibrated with an object of known size for each magnification, and the number of pixels was divided by the appropriate conversion factor. Exponential growth rates of *Arabidopsis* leaf expansion were calculated by linear regression analysis on log-transformed data of leaf area (mm^2) versus time. One-way analysis of variance (ANOVA) was performed to determine statistical significance between genotypes ($P \leq 0.05$) followed by a Bonferroni test to test for differences between group means at a 95% confidence interval (Microcal Origin Lab 7.5; Origin Lab).

Quantification of Variegation

The extent of leaf variegation in *im* seedlings was estimated nondestructively from images captured by a CCD camera (Retiga 1300 monochrome 10 bit; Qimaging) attached to a dissecting microscope (Leica Wild M3B) at 4, 10, and ×40 magnification as required. The camera was oriented directly over the center of the plant and the magnification selected on the dissecting microscope ensured that an image of the entire plant was captured for each measurement. Digital photos were analyzed using imaging analysis software (Northern Eclipse Image Analysis Software 7.0; Empix Imaging). The image analysis software was calibrated with an object of known size for each magnification, and the number of pixels was divided by the appropriate conversion factor. Images were then converted to grayscale, thereby creating a binary partitioning of the image intensities. An intensity value was determined, called the threshold value in order to separate green versus white sectors (Pham et al., 2000; Sezgin and Sankur, 2004). Threshold analysis was performed on each image captured to ensure that all green sectors could be clearly resolved from all white sectors irrespective of magnification. Total leaf area was measured by tracing and then calculating the area of each leaf per plant. Subsequently, the total area of white sectors per leaf was calculated and then divided by the total area of the leaf to determine the percentage of white sectors for each leaf examined. Statistical significance was determined by a one-way ANOVA at a 95% confidence interval, followed by a Bonferroni test to test for differences between group means (Microcal Origin Lab 7.5; Origin Lab).

Variegation during greening of wild-type and *im* etiolated cotyledons was assessed first by visual scoring of all cotyledons on each agar plate as either all green, all white, or variegated. Subsequently, this visual scoring of phenotype was verified by quantifying the total chlorophyll per germinated seedling from the same agar plates.

Chlorophyll Analyses

Chlorophyll was extracted from wild-type and *im* cotyledons with buffered 80% (v/v) aqueous acetone containing 2.5 mM sodium phosphate buffer, pH 7.8, and was measured by the method of Porra et al. (1989). The absorbance of the extracts was measured at 663.6 and 646.6 nm and corrected to 750 nm for light scattering in a Beckman DU-640 spectrophotometer (Beckman Coulter). Total chlorophyll was divided by the total number of seedlings. One-way ANOVA was performed to determine statistical significance between genotypes ($P \leq 0.05$) followed by a Bonferroni test to test for differences group means at a 95% confidence interval (Microcal Origin 7.5; Origin Lab).

Room Temperature Chlorophyll *a* Fluorescence

Light response curves and steady state fluorescence measurements were made using an Imaging PAM Chlorophyll Fluorometer (Heinz Walz). Samples were dark adapted for 20 min prior to all measurements. All fluorescence measurements were made at room temperature. The fluorescence parameters were calculated according to Schreiber et al. (1994). The maximum photochemical efficiency of PSII was calculated as F_v/F_m. Immediately after dark adaptation at room temperature, dark-adapted leaves and cotyledons were exposed to a short (800 ms) pulse of saturating blue light (6000 μmol photons m^{-2} s^{-1}; λ = 470 nm) provided by the Imaging PAM photodiode (IMAG-L; Heinz Walz). Nonphotochemical quenching was calculated as qN, and photochemical quenching was calculated as qP (Schreiber et al., 1994). The relative reduction state of PSII was calculated as 1-qP, which has been termed excitation pressure (Dietz et al., 1985; Hüner et al., 1998, 2003). Statistical significance was determined by a one-way ANOVA at a 95% confidence interval, followed by a Bonferroni test to test for differences between group means (Microcal Origin Lab 7.5; Origin Lab).

SDS-PAGE and Immunoblots

Whole plants from both wild-type and *im* genotypes were frozen in liquid nitrogen and ground to a fine powder. Total protein was extracted by the addition of 4% (w/v) SDS and heated for 20 min at 60°C in a water bath, with occasional mixing using a vortex. Total protein was measured using a BCA protein assay kit (Pierce) by measuring the change in absorbance at 562 nm using a Beckman DU-640 spectrophotometer (Beckman Coulter). Polypeptides were loaded on an equal protein basis of 20 μg protein and were separated on a 12% (w/v) SDS-PAGE according to the method of Laemmli (1970). Immunobloting was performed by electrophoretically transferring the proteins from SDS-PAGE gel to a nitrocellulose membrane (Bio-Rad Laboratories). Immunodetection was performed using horseradish peroxidase–conjugated secondary antibodies (Sigma-Aldrich) and enhanced chemiluminescence according to the manufacturer (ECL; Amersham-Pharmacia Biotech).

Wild-type and *im* seedlings germinated and grown to the cotyledon stage in the dark and subsequently exposed to CL of either 50 or 150 μmol photons m^{-2} s^{-1} at 25°C. Seedlings were harvested either in the dark (time 0) or at various times during the greening period up to 72 h, immediately frozen in liquid nitrogen, and ground to a fine powder. Samples were loaded on an equal protein basis (7 μg protein per lane) and were separated as previously described. Proteins were detected using specific polyclonal antibodies raised against protochlorophyllide oxidoreductase (POR) (1:1000 dilution; Agri-Sera), the light-harvesting complex associated with PSII (Lhcb2; 1:1000 dilution; Agri-Sera), PsbA and PsaB (1:2000 and 1:5000 dilution; Argi-Sera), and the large subunit of ribulose-1,5-bisphosphate carboxylase/oxygenase isolated from *Secale cereale* cv Musketeer (1:1000 dilution).

RNA Isolation, cDNA Synthesis, and Real-Time qRT-PCR

Wild-type and *im* seedlings were germinated and grown to the cotyledon stage on agar plates in the dark and subsequently exposed to CL of either 50 or 150 μmol photons m^{-2} s^{-1} at 25°C as described above. Seedlings were harvested either in the dark (time 0) or at various times during the greening period for up to a 24 h. Total RNA was extracted from these seedlings with the RNeasy plant mini kit (Qiagen). Total RNA (1 μg) was reverse transcribed with the high-capacity cDNA reverse transcriptase kit (Applied Biosystems). Real-time qPCR was performed using an Applied Biosystems 7900HT fast real time thermal cycler (Applied Biosystems) with primers designed for *IM*, *AOX1a*, *PHYA*, *PORA*, and an endogenous actin control gene, *ACT2*. The primers were designed between exon-exon boundaries to prevent amplification of genomic DNA. The primer sequences used are summarized in Supplemental Table 1 online. Quantitative analysis of gene expression was generated by the Power SYBR Green master mix kit (Applied Biosystems). Amplification for each gene was analyzed in the logarithmic phase. Relative quantification by comparative threshold cycle (C_T) analysis of *IM*, *AOX1a*, *PHYA*, and *PORA*

was performed against an internal standard (*ACT2*), and all samples were subtracted against a calibrator sample, wild type grown in the dark (0 h) at either 50 or 150 μmol photons m^{-2} s^{-1} depending on treatment. One-way ANOVA was performed to determine statistical significance between genotypes ($P \leq 0.05$) followed by a Bonferroni test to test for differences group means at a 95% confidence interval (Microcal Origin 7.5; Origin Lab).

Accession Numbers

Sequence data from this article can be found in the GenBank/EMBL data libraries and have the following Arabidopsis Genome Initiative locus identifiers: *ACT2*, At3g18780.2; *AOX1a*, At3g22370.1; *IM*, At4g22260.1; *PHYA*, At1g09570.1; *PORA*, At5g54190.1. Mutant lines used: *im* (CS3157; AT4G22260), *spotty* (AT4G22260), *var1* (CS271; AT5G42270), and *var2* (CS271; AT2G30950).

Supplemental Data

The following materials are available in the online version of this article.

Supplemental Figure 1. Growth Kinetics of Wild-Type and *im* Seedlings of *Arabidopsis*.

Supplemental Figure 2. The Effect of Growth Irradiance on the Light Response Curves for Excitation Pressure for *im* Plants Grown at 12°C.

Supplemental Figure 3. Extent of Variegation of the *var1*, *var2*, and *im* (*spotty*) Mutants of *Arabidopsis*.

Supplemental Figure 4. Representative Photographs of Wild-Type, *im*, *spotty*, *var1*, and *var2* Seedlings Grown under Short-Day Conditions (8 h Light/16 h Dark) at 12°C and an Irradiance of either 50, 150, or 450 μmol Photons m^{-2} s^{-1}.

Supplemental Figure 5. Biogenesis of Photosystem II and Photosystem I Reaction Centers.

Supplemental Figure 6. The Effects of an HL Pulse on the Greening in Wild-Type and *im* Cotyledons.

Supplemental Table 1. The Primers Designed for qRT-PCR for Genes from *Arabidopsis*.

ACKNOWLEDGMENTS

This work was supported by the Natural Sciences and Engineering Research Council of Canada (NSERC; individual discovery grants to D.P.M. and N.P.A.H.) and by the U.S. Department of Energy (Energy Biosciences; Grant DF-FG02-94ER20147 to S.R.R.). We thank Richard Harris of the Biotron Experimental Climate Change Research Center for his technical assistance in the development of the imaging technique. D.R. was the recipient of an NSERC postgraduate scholarship (CGS-D). S.W. was supported by an NSERC University Summer Research Assistantship.

Received August 25, 2008; revised September 22, 2009; accepted October 17, 2009; published November 6, 2009.

REFERENCES

Adams III, W.W., Demmig-Adams, B., Verhoeven, A.S., and Barker, D.H. (1995). 'Photoinhibition' during winter stress: involvement of sustained xanthophyll cycle-dependent energy dissipation. Aust. J. Plant Physiol. **22:** 261–276.

Aluru, M.R., Bae, H., Wu, D., and Rodermel, S.R. (2001). The Arabidopsis *immutans* mutation affects plastid differentiation and the morphogenesis of white and green sectors in variegated plants. Plant Physiol. **127:** 67–77.

Aluru, M.R., and Rodermel, S.R. (2004). Control of chloroplast redox by the IMMUTANS terminal oxidase. Physiol. Plant. **120:** 4–11.

Aluru, M.R., Yu, F., Fu, A., and Rodermel, S.R. (2006). Arabidopsis variegation mutants: New insights into chloroplast biogenesis. J. Exp. Bot. **57:** 1871–1881.

Aluru, M.R., Zola, J., Foudree, A., and Rodermel, S.R. (2009). Chloroplast photooxidation-induced transcriptome reprogramming in Arabidopsis *immutans* white leaf sectors. Plant Physiol. **150:** 904–923.

Arnholdt-Schmitt, B., Costab, J.H., and Fernandes de Melob, D. (2006). AOX – A functional marker for efficient cell reprogramming under stress? Trends Plant Sci. **11:** 281–287.

Bae, G., and Choi, G. (2008). Decoding of light signals by plant phytochromes and their interacting proteins. Annu. Rev. Plant Biol. **59:** 281–311.

Baker, N.R. (2008). Chlorophyll fluorescence: A probe of photosynthesis in vivo. Annu. Rev. Plant Biol. **59:** 89–113.

Barr, J., White, W.S., Chen, L., Bae, H., and Rodermel, S.R. (2004). The GHOST terminal oxidase regulates developmental programming in tomato fruit. Plant Cell Environ. **27:** 840–852.

Bellafiore, S., Barneche, F., Peltier, G., and Rochaix, J.-D. (2005). State transitions and light adaptation require chloroplast thylakoid protein kinase STN7. Nature **433:** 892–895.

Bennoun, P. (1982). Evidence for a respiratory chain in the chloroplast. Proc. Natl. Acad. Sci. USA **79:** 4352–4356.

Biswal, U.C., Biswal, B., and Raval, M.K. (2003). Chloroplast Biogenesis: From Plastid to Gerontoplast. (Dordrecht, The Netherlands: Kluwer Academic Publishers).

Bonardi, V., Pesaresi, P., Becker, T., Schleiff, E., Wagner, R., Pfannschmidt, T., Jahns, P., and Leister, D. (2005). Photosystem II core phosphorylation and photosynthetic acclimation require two different protein kinases. Nature **437:** 1179–1182.

Bräutigam, K., et al. (September 8, 2009). Dynamic plastid redox signals integrate gene expression and metabolism to induce distinct metabolic states in photosynthetic acclimation in *Arabidopsis*. Plant Cell http://dx.doi.org/10.1105/tpc.108.062018.

Carol, P., Stevenson, D., Bisanz, C., Breitenbach, J., Sandmann, G., Mache, R., Coupland, G., and Kuntz, M. (1999). Mutations in the *Arabidopsis* gene *IMMUTANS* cause a variegated phenotype by inactivating a chloroplast terminal oxidase associated with phytoene desaturation. Plant Cell **11:** 57–68.

Christie, J.M. (2007). Phototropin blue-light receptors. Annu. Rev. Plant Biol. **58:** 21–45.

Clifton, R., Millar, H.A., and Whelan, J. (2006). Alternative oxidases in Arabidopsis: A comparative analysis of differential expression in the gene family provides new insights into function of non-phosphorylating bypasses. Biochim. Biophys. Acta **1757:** 730–741.

Cournac, L., Redding, K., Ravenel, J., Rumeau, D., Josse, E.M., Kuntz, M., and Peltier, G. (2000). Electron flow between photosystem II and oxygen in chloroplasts of photosystem I-deficient algae is mediated by a quinol oxidase involved in chlororespiration. J. Biol. Chem. **275:** 17256–17262.

Cruz, J.L., Mosquim, P.R., Pelacani, C.R., Araújo, W.L., and DaMatta, F.M. (2003). Photosynthesis impairment in cassava leaves in response to nitrogen deficiency. Plant Soil **257:** 417–423.

Dietz, K.J. (2008). Redox signal integration: from stimulus to networks and genes. Physiol. Plant. **133:** 459–468.

Dietz, K.J., Schreiber, U., and Heber, U. (1985). The relationship between the redox state of Q_A and photosynthesis in leaves at various carbon-dioxide, oxygen and light regimes. Planta **166:** 219–226.

Eberhard, S., Finazzi, G., and Wollman, F.-A. (2008). The dynamics of photosynthesis. Annu. Rev. Plant Biol. **42:** 463–515.

Eckardt, N.A. (2007). Thylakoid development from biogenesis to senescence, and ruminations on regulation. Plant Cell **19:** 1135–1138.

Ensminger, I., Busch, F., and Hüner, N.P.A. (2006). Photostasis and cold acclimation: Sensing low temperature through photosynthesis. Physiol. Plant. **126:** 28–44.

Escoubas, J.M., Lomas, M., LaRoche, J., and Falkowski, P.G. (1995). Light intensity regulation of cab gene transcription is signaled by the redox state of the plastoquinone pool. Proc. Natl. Acad. Sci. USA **92:** 10237–10241.

Falkowski, P.G., and Chen, Y.-B. (2003). Photoacclimation of light harvesting systems in eukaryotic algae. In Advances in Photosynthesis and Respiration: Light-Harvesting Antennas in Photosynthesis, Vol. 13, B.R. Green and W.W. Parsons, eds (Dordrecht, The Netherlands: Kluwer Academic Publishers), pp. 423–447.

Fernández, A.P., and Strand, Å. (2008). Retrograde signalling and plant stress: Plastid signals initiate cellular stress responses. Curr. Opin. Plant Biol. **11:** 509–513.

Fu, A., Park, S., and Rodermel, S.R. (2005). Sequences required for the activity of IM (IMMUTANS), a plastid terminal oxidase. *In vitro* and *in planta* mutagenesis of iron-binding sites and a conserved sequence that corresponds to exon 8. J. Biol. Chem. **280:** 42489–42496.

Giraud, E., Ho, L.H.M., Clifton, R., Carroll, A., Estavillo, G., Tan, Y.-F., Howell, K.A., Ivanova, A., Pogson, B.J., Millar, A.H., and Whelan, J. (2008). The absence of ALTERNATIVE OXIDASE1a in Arabidopsis results in acute sensitivity to combined light and drought stress. Plant Physiol. **147:** 595–610.

Gray, G.R., Chauvin, L.-P., Sarhan, F., and Hüner, N.P.A. (1997). Cold acclimation and freezing tolerance. A complex interaction of light and temperature. Plant Physiol. **114:** 467–474.

Huang, C., He, W., Guo, J., Chang, X., Su, P., and Zhang, L. (2005). Increased sensitivity to salt stress in an ascorbate-deficient Arabidopsis mutant. J. Exp. Bot. **56:** 3041–3049.

Hüner, N.P.A., Öquist, G., and Sarhan, F. (1998). Energy balance and acclimation to light and cold. Trends Plant Sci. **3:** 224–230.

Hüner, N.P.A., Öquist, G., and Melis, A. (2003). Photostasis in plants, green algae and cyanobacteria: The role of light harvesting antenna complexes. In Advances in Photosynthesis and Respiration: Light-Harvesting Antennas in Photosynthesis, Vol. 13, B.R. Green and W.W. Parsons, eds (Dordrecht, The Netherlands: Kluwer Academic Publishers), pp. 401–421.

Joët, T., Genty, B., Josse, E.M., Kuntz, M., Cournac, L., and Peltier, G. (2002). Involvement of a plastid terminal oxidase in plastoquinone oxidation as enhanced by expression of the *Arabidopsis thaliana* enzyme in tobacco. J. Biol. Chem. **277:** 31623–31630.

Josse, E.M., Alcaraz, J.P., Labouré, A.M., and Kuntz, M. (2003). In vitro characterization of a plastid terminal oxidase (IM). Eur. J. Biochem. **270:** 3787–3794.

Josse, E.M., Simkin, A.J., Gaffé, J., Labouré, A.M., Kuntz, M., and Carol, P. (2000). A plastid terminal oxidase associated with carotenoid desaturation during chromoplast differentiation. Plant Physiol. **123:** 1427–1436.

Kargul, J., and Barber, J. (2008). Photosynthetic acclimation: Structural reorganisation of light harvesting antenna – role of redox-dependent phosphorylation of major and minor chlorophyll a/b binding proteins. FEBS Lett. **275:** 1056–1068.

Kramer, D.M., Johnson, G., Kiirats, O., and Edwards, G.E. (2004). New fluorescence parameters for the determination of Q_A redox state and excitation energy fluxes. Photosynth. Res. **79:** 209–218.

Krause, G.H., and Weis, E. (1991). Chlorophyll fluorescence and photosynthesis: The basics. Annu. Rev. Plant Physiol. Plant Mol. Biol. **42:** 313–349.

Krol, M., Hüner, N.P.A., and McIntosh, A. (1987). Chloroplast biogenesis at cold hardening temperatures. Development of photosystem I and photosystem II activities in relation to pigment accumulation. Photosynth. Res. **14:** 97–112.

Krol, M., Ivanov, A.G., Jansson, S., Kloppstech, K., and Hüner, N.P.A. (1999). Greening under high light or cold temperature affects the level of xanthophyll- cycle pigments, early light inducible proteins, and light-harvesting polypeptides in wild-type barley and the chlorina f2 mutant. Plant Physiol. **120:** 193–203.

Koussevitzky, S., Nott, A., Mockler, T.C., Hong, F., Sachetto-Martins, G., Surpin, M., Lim, J., Mittler, R., and Chory, J. (2007). Signals from chloroplasts converge to regulate nuclear gene expression. Science **316:** 715–719.

Laemmli, U. (1970). Cleavage of structural proteins during the assembly of the head of bacteriophage T4. Nature **227:** 680–685.

Li, Q.-H., and Yang, H.-Q. (2007). Cryptochrome signaling in plants. Photochem. Photobiol. **83:** 94–101.

Maxwell, D.P., Falk, S., and Hüner, N.P.A. (1994). Growth at low temperature mimics high light acclimation in *Chlorella vulgaris.* Plant Physiol. **105:** 535–543.

Maxwell, D.P., Falk, S., and Hüner, N.P.A. (1995a). Photosystem II excitation pressure and development of resistance to photoinhibition. Light-harvesting complex II abundance and zeaxanthin content in *Chlorella vulgaris.* Plant Physiol. **107:** 687–694.

Maxwell, D.P., Laudenbach, D.E., and Hüner, N.P.A. (1995b). Redox regulation of light-harvesting complex II and *cab* mRNA abundance in *Dunaliella salina.* Plant Physiol. **109:** 787–795.

Maxwell, D.P., Wang, Y., and McIntosh, L. (1999). The alternative oxidase lowers mitochondrial reactive oxygen production in plant cells. Proc. Natl. Acad. Sci. USA **96:** 8271–8276.

McCourt, P., and Keith, K. (1998). Sterile techniques in Arabidopsis. In Arabidopsis Protocols, J.M. Martinez-Zapater and J. Salinas, eds (Totowa, NJ: Humana Press), pp. 13–17.

McDonald, A.E. (2008). Alternative oxidase: An inter-kingdom perspective on the function and regulation of this broadly distributed 'cyanide-resistant' terminal oxidase. Funct. Plant Biol. **35:** 535–552.

Meskauskiene, R., Nater, M., Goslings, D., Kessler, F., op den Camp, R., and Apel, K. (2001). FLU: A negative regulator of chlorophyll biosynthesis in *Arabidopsis thaliana*. Proc. Natl. Acad. Sci. USA **98:** 12826–12831.

Minai, L., Wostrikoff, K., Wollman, F.-A., and Choquet, Y. (2006). Chloroplast biogenesis of photosystem II cores involves a series of assembly-controlled steps that regulate translation. Plant Cell **18:** 159–175.

Miskiewicz, E., Ivanov, A.G., Williams, J.P., Khan, M.U., Falk, S., and Hüner, N.P.A. (2000). Photosynthetic acclimation of the filamentous cyanobacterium, *Plectonema boryanum* UTEX 485, to temperature and light. Plant Cell Physiol. **41:** 767–775.

Miskiewicz, E., Ivanov, A.G., and Hüner, N.P.A. (2002). Stoichiometry of the photosynthetic apparatus and phycobilisome structure of the cyanobacterium *Plectonema boryanum* UTEX 485 are regulated by both light and temperature. Plant Physiol. **130:** 1414–1425.

Miura, E., Kato, Y., Matsushima, R., Albrecht, V., Laalami, S., and Sakamoto, W. (2007). The balance between protein synthesis and degradation in chloroplasts determines leaf variegation in *Arabidopsis yellow variegated* mutants. Plant Cell **19:** 1313–1328.

Mochizuki, N., Tanaka, R., Tanaka, A., Masuda, T., and Nagatani, A. (2008). The steady-state level of Mg-protoporphyrin IX is not a determinant of plastid-to-nucleus signaling in Arabidopsis. Proc. Natl. Acad. Sci. USA **105:** 15184–15189.

Moulin, M., McCormac, A., Terry, M.J., and Smith, A.G. (2008). Tetrapyrrole profiling in Arabidopsis seedlings reveals that retrograde

plastid nuclear signaling is not due to Mg-protoporphyrin IX accumulation. Proc. Natl. Acad. Sci. USA **105:** 15178–15183.

Murchie, E.H., Pinto, M., and Horton, P. (2009). Agriculture and the new challenges for photosynthesis research. New Phytol. **181:** 532–552.

Niyogi, K.K. (2000). Safety valves for photosynthesis. Curr. Opin. Plant Biol. **3:** 455–460.

Noctor, G., De Paepe, R., and Foyer, C.H. (2007). Mitochondrial redox biology and homeostasis in plants. Trends Plant Sci. **12:** 125–134.

op den Camp, R., Przybyla, D., Ochsenbein, C., Laloi, C., Kim, C., Danon, A., Wagner, D., Hideg, E., Göbel, C., Feussner, I., Nater, M., and Apel, K. (2003). Rapid induction of distinct stress responses after the release of singlet oxygen in *Arabidopsis*. Plant Cell **15:** 2320–2332.

Palatnik, J.F., Tognetti, V.B., Poli, H.O., Rodríguez, R.E., Blanco, N., Gattuso, M., Hajirezaei, M.-R., Sonnewald, U., Valle, E.M., and Carrillo, N. (2003). Transgenic tobacco plants expressing antisense ferredoxin-NADP(H) reductase transcripts display increased susceptibility to photo-oxidative damage. Plant J. **35:** 332–341.

Peltier, G., and Cournac, L. (2002). Chlororespiration. Annu. Rev. Plant Biol. **53:** 523–550.

Pesaresi, P., Hertle, A., Pribil, M., Kleine, T., Wagner, R., Strissel, H., Ihnatowicz, A., Bonardi, V., Scharfenberg, M., Schneider, A., Pfannschmidt, T., and Leister, D. (2009). *Arabidopsis* STN7 kinase provides a link between short- and long-term photosynthetic acclimation. Plant Cell **21:** 2402–2423.

Pfannschmidt, T., Nilsson, A., and Allen, J.F. (1999). Photosynthetic control of chloroplast gene expression. Nature **397:** 625–628.

Pfannschmidt, T. (2003). Chloroplast redox signals: How photosynthesis controls its own genes. Trends Plant Sci. **8:** 33–41.

Pfannschmidt, T., Bräutigam, K., Wagner, R., Dietzel, L., Schröter, Y., Steiner, S., and Nykytenko, A. (2009). Potential regulation of gene expression in photosynthetic cells by redox and energy state: approaches towards better understanding. Ann. Bot. (Lond.) **103:** 599–607.

Pham, D.L., Xu, C., and Prince, J.L. (2000). Current methods in medical image segmentation. Annu. Rev. Biomed. Eng. **2:** 315–337.

Philippar, K., Geis, T., Ilkavets, I., Oster, U., Schwenkert, S., Meurer, J., and Soll, J. (2007). Chloroplast biogenesis: The use of mutants to study the etioplast- chloroplast transition. Proc. Natl. Acad. Sci. USA **104:** 678–683.

Porra, R.J., Thompson, W.A., and Kreidemann, P.E. (1989). Determination of accurate extinction coefficients and simultaneous equations for assaying chlorophylls a and b extracted with different solvents: Verification of the concentration of chlorophyll standards by atomic absorption spectroscopy. Biochim. Biophys. Acta **975:** 384–394.

Rédei, G.P. (1963). Somatic instability caused by a cysteine-sensitive gene in Arabidopsis. Science **139:** 767–769.

Rédei, G.P. (1975). Arabidopsis as a genetic tool. Annu. Rev. Genet. **9:** 111–127.

Röbbelen, G. (1968). Genbedingte rotlicht-empfindlichkeit der chloroplastendifferenzierung bei Arabidopsis. Planta **80:** 237–254.

Rodermel, S.R. (2001). Pathways of plastid to nucleus signaling. Trends Plant Sci. **6:** 471–478.

Rodermel, S.R. (2002). Arabidopsis variegation mutants. In The Arabidopsis Book, C.R. Somerville and E.R. Myerowitz, eds (Rockville, MD: American Society of Plant Biologists), pp. 1–28.

Rochaix, J.-D. (2004). Genetics of the biogenesis and dynamics of the photosynthetic machinery in eukaryotes. Plant Cell **16:** 1650–1660.

Rockwell, N.C., Su, Y.-S., and Lagarias, J.C. (2006). Phytochrome structure and signaling mechanisms. Annu. Rev. Plant Biol. **57:** 837–858.

Rosso, D., Ivanov, A.G., Fu, A., Geisler-Lee, J., Hendrickson, L., Geisler, M., Stewart, G., Krol, M., Hurry, V., Rodermel, S.R., Maxwell, D.P., and Hüner, N.P.A. (2006). IMMUTANS does not act as a stress-induced safety valve in the protection of the photosynthetic apparatus of Arabidopsis during steady-state photosynthesis. Plant Physiol. **142:** 1–12.

Ruckle, M.E., DeMarco, S.M., and Larkin, R.M. (2007). Plastid signals remodel light signaling networks and are essential for efficient chloroplast biogenesis in Arabidopsis. Plant Cell **19:** 3944–3960.

Sakamoto, W., Miyagishima, S., and Jarvis, P. (July 22, 2008). Chloroplast biogenesis: Control of plastid development, protein import, division and inheritance. In The Arabidopsis Book, C.R. Somerville and E.M. Meyerowitz, eds (Rockville, MD: American Society of Plant Biologists), doi/10.1199/tab.0110, http://www.aspb.org/publications/arabidopsis/.

Schreiber, U., Bilger, W., and Neubauer, C. (1994). Chlorophyll fluorescence as a non-intrusive indicator for rapid assessment of in vivo photosynthesis. In Ecophysiology of Photosynthesis, E. Schulze and M.M. Caldwell, eds (Berlin: Springer-Verlag), pp. 49–70.

Sezgin, M., and Sankur, B. (2004). Survey over image thresholding techniques and quantitative performance evaluation. J. Electron. Imaging **13:** 146–165.

Shahbazi, M., Gilbert, M., Labouré, A., and Kuntz, M. (2007). The dual role of the plastid terminal oxidase (PTOX) in tomato. Plant Physiol. **145:** 691–702.

Stepien, P., and Johnson, G.N. (2009). Contrasting responses of photosynthesis to salt stress in the glycophyte *Arabidopsis thaliana* and the halophyte *Tellungiella halophila*. Role of the plastid terminal oxidase as an alternative electron sink. Plant Physiol. **149:** 1154–1165.

Strand, Å., Asami, T., Alonso, J., Ecker, J.R., and Chory, J. (2003). Chloroplast to nucleus communication triggered by accumulation of Mg-protoporphyrinIX. Nature **421:** 79–83.

Streb, P., Josse, E.-M., Gallouet, E., Baptist, F., Kuntz, M., and Cornic, G. (2005). Evidence for alternative electron sinks to photosynthetic carbon assimilation in the high mountain plant species *Ranunculus glacialis.* Plant Cell Environ. **28:** 1123–1135.

Sun, S.-Y., Chao, D.Y., Li, X.-M., Shi, M., Gao, J.-P., Zhu, M.-Z., Yang, S.L., and Lin, H.-X. (2009). OsHAL3 mediates a new pathway in the light-regulated growth of rice. Nat. Cell Biol. **11:** 845–851.

Tobin, E.M., and Silverthorne, J. (1985). Light regulation of gene expression in higher plants. Annu. Rev. Plant Physiol. **36:** 569–593.

Umbach, A.L., Ng, V.S., and Siedow, J.N. (2006). Regulation of plant alternative oxidase activity: A tale of two cysteines. Biochim. Biophys. Acta **757:** 135–142.

Vanlerberghe, G.C., and McIntosh, L. (1997). Alternative oxidase: From gene to function. Annu. Rev. Plant Physiol. Plant Mol. Biol. **48:** 703–734.

Vogelmann, T.C., Nishio, J.N., and Smith, W.K. (1996). Leaves and light capture: light propagation and gradients of carbon fixation within leaves. Trends Plant Sci. **1:** 65–70.

Wetzel, C.M., Jiang, C.Z., Meehan, L.J., Voytas, D.F., and Rodermel, S.R. (1994). Nuclear-organelle interactions: The *immutans* variegation mutant of *Arabidopsis* is plastid autonomous and impaired in carotenoid biosynthesis. Plant J. **6:** 161–175.

Wilson, K.E., and Hüner, N.P.A. (2000). The role of growth rate, redox-state of the plastoquinone pool and the trans-thylakoid ΔpH in photoacclimation of *Chlorella vulgaris* to growth irradiance and temperature. Planta **212:** 93–102.

Wilson, K.E., Krol, M., and Hüner, N.P.A. (2003). Temperature-induced

greening of *Chlorella vulgaris*. The role of the cellular energy balance and zeaxanthin-dependent nonphotochemical quenching. Planta **217:** 616–627.

Wilson, K.E., Ivanov, A.G., Öquist, G., Grodzinski, B., Sarhan, F., and Hüner, N.P.A. (2006). Energy balance, organellar redox status, and acclimation to environmental stress. Can. J. Bot. **84:** 1355–1370.

Woodson, J.D., and Chory, J. (2008). Coordination of gene expression between organellar and nuclear genomes. Nat. Rev. Genet. **9:** 383–395.

Wu, D., Wright, D.A., Wetzel, C.M., Voytas, D.F., and Rodermel, S.R. (1999). The IMMUTANS variegation locus of *Arabidopsis* defines a mitochondrial alternative oxidase homolog that functions during early chloroplast biogenesis. Plant Cell **11:** 43–55.

Yu, F., Fu, A., Aluru, M., Park, S., Xu, Y., Liu, H., Liu, X., Foudree, A., Nambogga, M., and Rodermel, S.R. (2007). Variegation mutants and mechanisms of chloroplast biogenesis. Plant Cell Environ. **30:** 350–365.